HHS Public Access

Author manuscript

J Mol Cell Cardiol. Author manuscript; available in PMC 2024 June 01.

Published in final edited form as:

J Mol Cell Cardiol. 2023 June ; 179: 90–101. doi:10.1016/j.yjmcc.2023.04.004.

The Role of P21-Activated Kinase (Pak1) in Sinus Node Function

Carlos H. Pereira[a,b], **Dan J. Bare**[c], **Paola C. Rosas**[d], **Fernando A.L. Dias**[b], **Kathrin Banach**[a]

[a]Dept. of Internal Medicine/Cardiology, Rush University Medical Center, 1750 W. Harrison St., Chicago, IL 60612, USA

[b]Biological Science Center, Department of Physiology, Av. Cel Francisco H. dos Santos 100, 19031 Centro Politécnico-Curitiba, PR-Brasil

[c]Dept. of Physiology & Biophysics, The Ohio State University, 5018 Graves Hall, 333 W.10th Ave. Columbus, Ohio 4321, USA

[d]Dept. of Pharmacy Practice, College of Pharmacy, 833 S Wood St., Chicago, IL 60612, USA

Abstract

Sinoatrial node (SAN) dysfunction (SND) and atrial arrhythmia frequently occur simultaneously with a hazard ratio of 4.2 for new onset atrial fibrillation (AF) in SND patients. In the atrial muscle attenuated activity of p21-activated kinase 1 (Pak1) increases the risk for AF by enhancing NADPH oxidase 2 dependent production of reactive oxygen species (ROS). However, the role of Pak1 dependent ROS regulation in SAN function has not yet been determined. We hypothesize that Pak1 activity maintains SAN activity by regulating the expression of the hyperpolarization activated cyclic nucleotide gated cation channel (HCN).

To determine Pak1 dependent changes in heart rate (HR) regulation we quantified the intrinsic sinus rhythm in wild type (WT) and Pak1 deficient ($Pak1^{-/-}$) mice of both sexes in vivo and in isolated Langendorff perfused hearts. $Pak1^{-/-}$ hearts displayed an attenuated HR in vivo after autonomic blockage and in isolated hearts. The contribution of the Ca^{2+} clock to pacemaker activity remained unchanged, but Ivabradine (3 μM), a blocker of HCN channels that are a membrane clock component, eliminated the differences in SAN activity between WT and $Pak1^{-/-}$ hearts. Reduced HCN4 expression was confirmed in $Pak1^{-/-}$ right atria. The reduced HCN activity in $Pak1^{-/-}$ could be rescued by class II HDAC inhibition (LMK235), ROS scavenging (TEMPOL) or attenuation of Extracellular Signal-Regulated Kinase (ERK) 1/2 activity (SCH772984). No sex specific differences in Pak1 dependent SAN regulation were determined.

Our results establish Pak1 as a class II HDAC regulator and a potential therapeutic target to attenuate SAN bradycardia and AF susceptibility.

[*]**Corresponding Author:** Kathrin Banach, Ph.D., Dept. of Internal Medicine/Cardiology, Rush University, 1750 W. Harrison St., Jelke Bldg. Room 1419, Chicago, IL 60612-3833, Phone: 312-563-3553, kathrin_banach@rush.edu.

Declaration of Competing Interests:
The authors have no competing interests.

Graphical Abstract

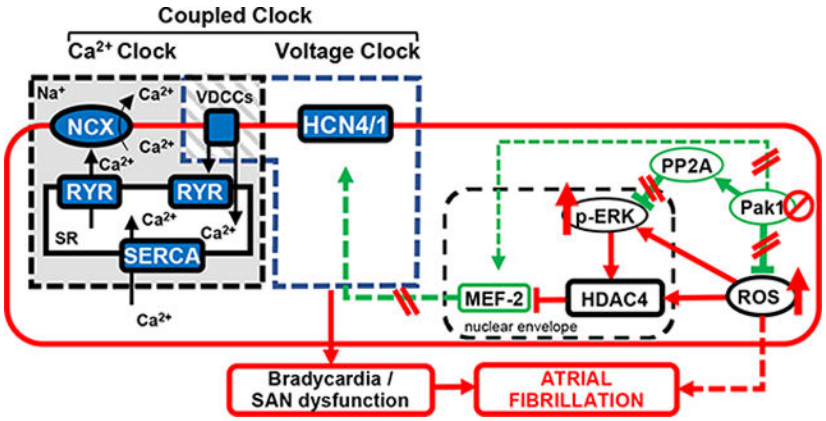

Keywords

Sinoatrial node; membrane clock; HCN channel; p21-activated kinase 1; atrial fibrillation; reactive oxygen species

Introduction

The heart's pacemaker, the sinoatrial node (SAN), consists of specialized muscle fibers that rhythmically generate electrical activity. This basal automaticity or intrinsic sinus rhythm (SR) is under constant control of the autonomic nervous system (ANS). SAN bradycardia, a manifestation of sinus node dysfunction (SND), describes the inability of the heart's natural pacemaker to generate cardiac excitation at an appropriate frequency [1]. SND and atrial arrhythmia frequently coincide [1–3] and SND itself increases the hazard ratio for atrial fibrillation (AF) by promoting dispersion of repolarization, reentry, and atrial ectopy [4–6]. In patients with AF and animal models of atrial tachyarrhythmia on the other hand, SAN automaticity is attenuated but can recover after cardioversion indicating an arrhythmia induced remodeling of the pacemaker mechanism [5,7,8].

The SAN pacemaker cells exhibit distinct electrophysiological and calcium (Ca^{2+}) handling properties that allow them to rhythmically generate action potentials (APs). Due to the scarcity of the inward rectifier potassium (K^+) channel (I_{K1}, Kir2.1 – 2.4), SAN cells exhibit a depolarized maximum diastolic potential and a progressive depolarization of the resting membrane potential (V_m) during diastole (diastolic depolarization). The diastolic depolarization is driven by two coupled cellular pacemaker mechanisms that have been termed the Ca^{2+}- and membrane- clock [1,9,10]. Due to their coordinated action and interdependence, they make up the coupled-clock mechanism.

The contribution of the Ca^{2+} clock to SAN pacemaker activity depends on the release of Ca^{2+} from the sarcoplasmic reticulum through the activation of ryanodine or inositol 1,4,5-tris phosphate receptor (RyR and IP_3R, respectively) channels [9–12]. These release events that increase in frequency toward the end of diastole [12,13], are translated into a depolarization of V_m by the electrogenic sodium-calcium exchanger (NCX) which in the

forward mode extrudes one Ca^{2+} ion by bringing 3 Na^{+} ions into the cell [11,13–15]. The rate of depolarization by the Ca^{2+} clock depends on the interplay between the Ca^{2+}-load of the SR, the open probability of the Ca^{2+} release channels, as well as the expression and activity of NCX [10,16]. One driver of the membrane clock is the pacemaker current (I_f) through the hyperpolarization-activated, cyclic-nucleotide gated cation channel (HCN) [4,17–19]. The current is activated upon repolarization, counters further hyperpolarization of V_m, and contributes to the early phase of the diastolic depolarization [4,17]. Of the 4 HCN protein isoforms identified, HCN4 predominates in the human and rodent SAN and its deletion in animal models leads to a significant reduction of I_f, SAN bradycardia, and frequent sinus pauses [18,20,21]. In humans, loss of function mutations in the HCN4 channel or its auxiliary proteins have been associated with SAN bradycardia as well as AF, AV-block, and tachy-bradycardia [20,22,23]. In addition, voltage-dependent Ca^{2+} channels (VDCCs), tetrodotoxin (TTX)-sensitive Na^{+} channels ($I_{Na,TTX}$) [24,25], as well as transient receptor potential (TRPM and TRPC)[26] channels have been shown to contribute to the membrane clock. The T- type ($Ca_v3.1$) and L-type ($Ca_v1.2$, $Ca_v1.3$) channels expressed in SAN tissue, not only contribute to the membrane clock by furthering the depolarization, but also critically modulate the Ca clock mechanism. VDCC dependent Ca influx regulates the SR load and thereby the RyR open probability, and the frequency of the spontaneous Ca release events [13,27–29].

The serine/threonine protein kinase p21-activated kinase (Pak1), activated by Ras related small G-protein, exerts cardioprotective signaling [30–35]. Pak1 attenuates cardiac hypertrophic remodeling by counteracting mitogen-activated protein kinase (MAPK) activity [34] and in atrial and ventricular myocytes we demonstrated that Pak1 regulates the production of reactive oxygen species (ROS) by antagonizing the activity of the nicotinamide adenine dinucleotide phosphate (NADPH) oxidase 2 (NOX2). Attenuation of Pak1 activity consequently increases cellular ROS production and the propensity for arrhythmic Ca^{2+} release in the atria and ventricle after ischemia reperfusion injury [33,35].

A ROS dependent remodeling of SAN pacemaker activity has been described in animal models of hypertension [36,37], diabetes [38], ischemia reperfusion [39], and cardiomyopathy [40]. The disease induced SAN bradycardia was shown to be a consequence of enhanced NOX2 as well as mitochondrial ROS production [36,39,40]. The ROS mediated reduction in pacemaker function was attributed to altered activity of the Ca^{2+} calmodulin kinase II (CaMKII) [37,41] and a subsequent increase in pacemaker cell apoptosis or a reduction in RyR open probability and subsequent attenuation of Ca^{2+} clock activity, respectively. As an alternative mechanism, a ROS dependent increase in class II histone deacetylase 4 (HDAC4) activity was linked to attenuated HCN4 protein expression [40]. Pak1 can regulate cardiac pacemaker activity by counteracting the positive chronotropic effect of β-adrenergic stimulation through activation of its downstream target protein phosphatase 2A (PP2A) and the reduction of L-type Ca^{2+} channel and inwardly rectifying K^{+}-channel activity [42]. Under physiological conditions however, when the heart rate (HR) is under the influence of the ANS, no differences in pacemaker activity were determined between WT and $Pak1^{-/-}$ animals [34,35]. The impact of Pak1 on SAN function in the absence of ANS control has yet to be determined. Since loss of Pak1 activity increases the susceptibility for AF and SAN dysfunction can be the cause and consequence of AF, in the

current study, we aimed to determine the role of Pak1 in the regulation of cardiac pacemaker activity. In vivo, in the whole heart, and on the cellular level we tested the hypothesis, that Pak1 maintains SAN activity by regulating the expression of HCN through attenuation of NOX2 dependent ROS production and suppression of class II HDAC activity.

2. Material and Methods

2.1 Animals

Hearts were isolated from 3- to 6-month-old male and female WT (FVB/N; The Jackson Laboratory, Bar Harbor, ME USA) and Pak1 deficient mice ($Pak1^{-/-}$) [31,33,35]. Animals were maintained at a 12–12-hour light-dark cycle and food and water were provided *ad libitum*. To determine the role of class II HDACs, ROS production and β-adrenergic signaling in the remodeling of SAN function, WT and $Pak1^{-/-}$ animals were treated with either class II HDAC inhibitor LMK235 (intraperitoneal (IP) injections, 5 mg/kg/day for 3 days) [43], the ROS scavenger 4-hydroxy-2,2,6,6-tetramethylpiperidin-1-oxyl (TEMPOL: 2 mmol/L supplemented drinking water, 3 days) [44], the β-blocker atenolol (IP, twice a day at 2.5 mg/kg for 3 days) [45], or the Extracellular Signal-Regulated Kinase 1/2 (ERK1/2) inhibitor SCH772984 (ERK_i: IP, 25 mg/kg/day for 3 days) [46], respectively.

All animal procedures were performed with the approval of the IACUC of Rush University and in accordance with the National Institute of Health's Guide for the Care and Use of Laboratory Animals.

2.2 Electrocardiogram (ECG) recordings

ECG recordings were performed in isoflurane anesthetized mice (induction: 4 %; maintenance: 2 %; O_2: 0.8 – 1.0 L/min) using an Indus Mouse Surgical Monitor (Indus Instruments). Data were digitized (4 kHz; PowerLab 8/30, AD instruments, Colorado Springs, USA) and analyzed using LabChart 8 (AD instruments, Colorado Springs, USA). ECGs were recorded continuously during an adaptation period (10 min) and after intraperitoneal injection of atropine (1 mg/kg) and/or propranolol (1 mg/kg). HR was quantified from ECG recordings when a new steady state was reached, approximately 10 min after the injection. All ECG recordings were performed between 8 – 10 am to minimize circadian variation in the HR and SAN ion channel expression [47].

2.3 Isolated Langendorff Perfused Hearts

Mouse hearts were isolated, connected to a Langendorff perfusion system (Harvard Apparatus, Holliston, USA), and continuously perfused with Krebs-Hänseleit solution containing (mmol/L): NaCl 119, KCl 4, KH_2PO_4 1.2, $NaHCO_3$ 25, Glucose 10, Na Pyruvate 2, $MgSO_4$ 2, $CaCl_2$ 1.8; at 37°C, 95% O_2-5% CO_2, pH of 7.4) [35]. Atrial electrograms were recorded using bipolar electrodes (Harvard Apparatus) or multielectrode arrays (FlexMEA36; Multichannel Systems, Reutlingen, Germany) placed on the left atrial epicardial surface. Atrial electrograms were recorded continuously during an adaptation period (15 min) and the perfusion of pharmacological compounds (cyclopiazonic acid (CPA): 5 μmol/L [16], ivabradine (IVA): 3 μmol/L [48], tertiapin-q (TerQ): 0.3 μmol/L [49], or carbachol (CCh): 0.1 to 0.8 μmol/L) [50]. Bipolar electrograms were recorded using

PowerLab 8/30 supplemented with an animal BioAmp (ML136) and analyzed in LabChart 8 (AD Instruments, Colorado Springs, USA). The channels were amplified and sampled at 4 kHz, at a range of ±10 mV.

2.4 AF inducibility

Sinus rhythm (SR) from spontaneously beating hearts in the Langendorff configuration was interrupted by burst pacing episodes (15 times 2 s at 50 Hz) applied to the right atrium[35]. Arrhythmic activity was quantified as the % of hearts with atrial fibrillation (AF: spontaneous atrial arrhythmic activity longer than 1 s) [35].

2.5 Quantification of reactive oxygen species (ROS) production

Cellular ROS production was quantified in atrial myocytes isolated from WT and $Pak1^{-/-}$ hearts as previously described [35,51]. In short, hearts were excised, connected to a Langendorff apparatus, and perfused with Ca^{2+}-free tyrode solution supplemented with 2,3-Butanedione monoxime (0.5 μmol/L) and a digestion solution supplemented with $CaCl_2$ (12.7 μmol/L), Liberase blendzyme (60 μg/mL), Trypsin (0.014 %), and Phenol red (0.5 %). For further digestion, atria were removed and placed into protease (1 mg/mL) solution. The digestion was stopped by addition of bovine calf serum (Hyclone) before extracellular Ca^{2+} was raised to 1 mmol/L. To quantify the production of ROS isolated atrial myocytes were loaded with 2′,7′-dichlorofluorescein diacetate (DCFH) (10 μmol/L for 30 min at 37 °C) as previously described. DCF fluorescence was monitored (excitation: ~492–495 nm, emission: 517–527 nm) every 2 minutes for a period of 18 minutes. The fluorescent signal was normalized to the fluorescence at the onset of the experiment (F0) and quantified as the change in fluorescence over time [33,35].

2.6 HL-1 Cell Culture, SDS-PAGE and Immunoblotting

The atrial myocyte cell line (HL-1 cells) was cultured and propagated as previously described [33,52,53]. For the experiments cells were grown to confluency in cell culture dishes before treatment with Pak1-siRNA (48 h) [31,35]. At the end of the treatment period HL-1 cells were lysed directly with the addition of hot 1-X Laemmli sample buffer without β-mercaptoethanol (β-ME) or bromophenol blue dye and heated to 95 °C for 5 min. Sample protein determinations were made with a BCA protein assay kit (Pierce) and then β-ME and dye were added to the final concentrations for 1-X sample buffer and heated as before. Cell lysates were separated by using pre-cast 4–20% Novex tris-glycine gels (Invitrogen) following standard electrophoresis protocols for SDS-PAGE and immunoblotting as previously described [33,35,54]. Typically, 10–45 μg of protein were loaded per well. Primary antibodies used for Western blotting were directed against the HCN4 (APC-052, Alomone labs), β-Actin (No. 4970, Cell Signaling), phopho-ERK1/2 (*p*-ERK1/2; No. 4370; Cell Signaling), phospho-p38 (*p*-p38; No. 4511, Cell Signaling), and GAPDH (No. 5174, Cell Signaling). Species-specific horseradish peroxidase-conjugated secondary antibodies were used and visualization was accomplished by using Western Lighting chemi-luminescence reagents (PerkinElmer) and Kodak BioMax film.

2.7 Chemicals

All reagents were purchased from Sigma Aldrich except for CPA (Tocris Bioscience), TEMPOL (Calbiochem), LiberaseTM (Roche), CM-H2DCF-DA (Thermo Fisher), LMK235 (Cayman Chemical), and SCH772984 (Cayman Chemical).

2.8 Statistic

A Shapiro-Wilk test was performed to assess the normality of the data. Data are expressed as mean ± standard deviation (SD). Comparisons were made using a student's t-test or 1-way ANOVA followed by Tukey's multiple comparison test. When the Shapiro-Wilk test revealed a non-parametric distribution, the hypothesis tests Mann-Whitney test and Kruskal Wallis ANOVA were used. For ROS experiments a nested t-test or nested One Way ANOVA was used. The level of significance was set at $p<0.05$.

3. Results

3.1 Intrinsic Heart Rate

In SAN cells the stimulation of Pak1 attenuates the response to β-adrenergic stimulation [42] however, loss of Pak1 in vivo, did not alter the sinus rhythm (SR). To quantify the intrinsic HR independent from ANS regulation, we recorded ECGs under isoflurane anesthesia from male and female WT and Pak1$^{-/-}$ mice under basal conditions and after ANS block. Parasympathetic signaling was suppressed with the muscarinic receptor blocker atropine (1 mg/kg) whereas sympathetic signaling was attenuated with the β-adrenergic receptor blocker propranolol (1 mg/kg). Under basal conditions no difference in HR was determined between WT and Pak1$^{-/-}$ animals of either sex (Fig. 1Aa,Ab: WT$_{♂}$: 450.4 ± 26.8 bpm, n = 16; Pak1$^{-/-}{}_{♂}$: 440.4 ± 24.1, n = 13; p=0.734; WT$_{♀}$: 429.2 ± 28.7, n = 16; Pak1$^{-/-}{}_{♀}$: 430.8 ± 23.1 bpm, n = 12; $p = 0.998$). Suppression of ANS signaling (atropine + propranolol) attenuated the intrinsic HR and revealed a reduced frequency in male and female Pak1$^{-/-}$ animals compared to their WT counterparts (Fig. 1Ba,Bb: WT$_{♂}$: 399.0 ± 32.2 bpm, n = 16; Pak1$^{-/-}{}_{♂}$: 365.5 ± 34.9, n = 13; p<0.014; WT$_{♀}$: 396.3 ± 13.9, n = 13; Pak1$^{-/-}{}_{♀}$: 357.4 ± 24.8 bpm, n = 8; $p = 0.018$). The difference in the intrinsic HR between WT and Pak1$^{-/-}$ mice of both sexes was confirmed in isolated Langendorff perfused hearts where the spontaneous HR was recorded by bi-atrial electrograms or MEAs (Fig.1Ca,Cb: WT$_{♂}$: 343.7 ± 42.1 bpm, n = 24; Pak1$^{-/-}{}_{♂}$: 280.7 ± 31.9, n = 28; p<0.0001; WT$_{♀}$: 371.6 ± 43.8, n = 14; Pak1$^{-/-}{}_{♀}$: 308.2 ± 38.9, n = 12; $p = 0.0004$). Analysis of the PR-interval in Langendorff perfused hearts, paced at a constant frequency of 8 Hz further exposed a prolonged AV nodal conductance in Pak1$^{-/-}$ hearts (WT$_{♂}$: 33.9 ± 2.3 ms, n = 4; Pak1−/−$_{♂}$: 43.5 ± 5.7 ms, n = 4; p=0.038). The data support that loss of Pak1 attenuates the excitability of the conduction system thereby reducing the intrinsic SR.

To determine in vivo if the change in intrinsic HR is compensated by an altered activity of the ANS, atropine and propranolol induced changes in HR were quantified individually. Intra peritoneal injection of atropine induced a significant increase in HR in all animals, but the atropine induced change was significantly attenuated in Pak1$^{-/-}$ compared to WT animals of both sexes (Fig. 2A: WT$_{♂}$: 9.77 ± 5.04 %, n = 10; Pak1$^{-/-}{}_{♂}$: 4.64 ± 4.46 %, n = 9; p=0.031; WT$_{♀}$: 9.94 ± 7.39 %, n = 13; Pak1$^{-/-}{}_{♀}$: 0.40 ± 4.07 %, n = 8; p=0.003). The

percentage decrease in HR induced by propranolol was significantly larger in male $Pak1^{-/-}$ compared to WT animals (Fig. 2B: $WT_{♂}$: −13.51 ± 2.54 %, n = 6; $Pak1^{-/-}{}_{♂}$: −18.45 ± 1.56 %, n = 4, p = 0.009) but in WT and $Pak1^{-/-}$ female animals did not reach significance ($WT_{♀}$: −18.98 ± 5.42 %, n = 5; $Pak1^{-/-}{}_{♀}$: −23.72 ± 5.02 %, n = 6; p = 0.116). An increased propensity for AF, as seen in $Pak1^{-/-}$ animals has been linked to a chronic activation of the acetylcholine sensitive G-protein activated inwardly rectifying K-channel (GIRK) and a reduced acetylcholine induced change in GIRK activation [55,56]. Male WT and $Pak1^{-/-}$ Langendorff perfused hearts however, showed comparable changes in HR in response to increasing carbachol (CCh) concentrations (Fig. 2C: CCh: 100 – 800 nmol/L) and the GIRK channel blocker TerQ (Fig. 2D: $WT_{♂}$: −2.56 ± 7.25 %, n = 6; $Pak1^{-/-}{}_{♂}$: 3.90 ± 6.16 %, n = 7; p = 0.110). The data suggests that in vivo, the attenuated SAN function in $Pak1^{-/-}$ animals is compensated for by an altered autonomic tone.

3.2 Calcium Clock

In mouse SAN cells, Pak1 regulates the L-type Ca^{2+} current by activation of PP2A [42]. Changes in Ca^{2+} influx can modulate the contribution of the Ca^{2+} clock to pacemaker activity [10,13,27,57]. To quantify the contribution of the Ca^{2+} clock, isolated Langendorff perfused hearts from male and female WT and $Pak1^{-/-}$ mice were perfused with the SERCA blocker CPA (5 μmol/L) [16]. CPA, that leads to a depletion of the SR and elimination of the Ca^{2+} clock mechanism induced an attenuation in HR that was comparable between WT and $Pak1^{-/-}$ hearts of both sexes (Fig. 3Aab: $WT_{♂}$: −21.79 ± 10.81 %, n = 6; $Pak1^{-/-}{}_{♂}$: −21.66 ± 7.52 %, n = 5; p = 0.982; $WT_{♀}$: −22.03 ± 5.43 %, n = 3; $Pak1^{-/-}{}_{♀}$: −18.32 ± 4.07 %, n = 4; p = 0.345). However, the difference in HR between WT and $Pak1^{-/-}$ persisted in presence of CPA, but only reached significance for males (Fig. 3Ac: $WT_{♂}$: 329.6 ± 42.5 bpm, n = 6; $Pak1^{-/-}{}_{♂}$: 246.1 ± 23.8 bpm, n = 5; p=0.001; $WT_{♀}$: 295.2 ± 4.5 bpm, n = 3; $Pak1^{-/-}{}_{♀}$: 236.0 ± 7.4 bpm, n = 4; p=0.072). In an alternative approach we assessed the contribution of the Ca^{2+} clock by exposing Langendorff perfused hearts to caffeine (20 mmol/L)[58]. Caffeine, as a RyR agonist, induces Ca^{2+} release from the SR thereby transiently increasing HR. Subsequent depletion of the intracellular Ca^{2+} store eliminates the Ca^{2+} clock's contribution to pacemaker activity (Supplemental Fig. 1). Comparable to CPA, caffeine resulted in a comparable decrease in the HR in WT and $Pak1^{-/-}$ hearts but failed to eliminate the HR difference between the animals. Overall, the data imply that the Ca^{2+} clock contributes comparably to pacemaker activity in male and female WT and $Pak1^{-/-}$ mice.

3.3 Contribution of the Membrane Clock mechanism I_f

The pacemaker current (I_f) through HCN4 contributes to the early phase of the diastolic depolarization and represents one of the driving forces of the SAN membrane clock mechanism [4,27,57]. To determine the contribution of I_f in WT and $Pak1^{-/-}$ animals, isolated hearts were perfused with the I_f blocker IVA (3 μmol/L) [48]. IVA reduced the intrinsic HR in all hearts however, in both sexes the induced change was significantly smaller in $Pak1^{-/-}{}_{IVA}$ than in WT_{IVA} (Fig. 3Bab: $WT_{♂}$: −45.11 ± 6.35 %, n = 6; $Pak1^{-/-}{}_{♂}$: −19.30 ± 3.95 %, n = 6; p = 0.0001; $WT_{♀}$: −44.17 ± 8.76 %, n = 5; $Pak1^{-/-}{}_{♀}$: −22.02 ± 11.3 %, n = 6; p = 0.001) and the difference in the intrinsic HR was eliminated between WT_{IVA} and $Pak1^{-/-}{}_{IVA}$ hearts (Fig. 3Bc: $WT_{♂}$: 186.3 ± 43.2 bpm, n = 6; $Pak1^{-/-}{}_{♂}$: 244.2 ± 35.6 bpm, n = 6; p = 0.163; $WT_{♀}$: 205.4 ± 56.9 bpm, n = 5; $Pak1^{-/-}{}_{♀}$: 239.1 ± 47.8 bpm, n =

6; $p = 0.626$). Immunoblotting of protein isolated from the right atria of WT and Pak1$^{-/-}$ animals further revealed decreased HCN4 protein levels in Pak1$^{-/-}$ hearts (Fig. 3Ca,b). The data allude that loss of Pak1 attenuates the contribution of I_f/HCN to pacemaker activity.

The positive chronotropic effect of β-adrenergic stimulation depends in part on the cyclic-adenosine mono phosphate (cAMP) dependent regulation of HCN4. We mimicked β-adrenergic stimulation by perfusing isolated hearts with the adenylate cyclase (AC) activator forskolin (5 μmol/L). As l chronotropic response in Pak1$^{-/-}$ hearts (WT$_{♂}$: 15.73 ± 12.34 %, n = 10; Pak1$^{-/-}{}_{♂}$: 36.03 ± 15.05 %, n = 7; p=0.008; Supplemental Fig. 2). The IVA sensitive contribution to the HR however, remained significantly lower in Pak1$^{-/-}$ hearts (WT$_{♂}$: −39.34 ± 9.55 %, n = 4; Pak1$^{-/-}{}_{♂}$: −19.17 ± 2.84 %, n = 4; p=0.012) while the contribution of the Ca^{2+} clock in Pak1$^{-/-}$ now significantly exceeded that of WT hearts (WT$_{♂}$: −24.08 ± 9.29 %, n = 6; Pak1$^{-/-}{}_{♂}$: −38.70 ± 7.87 %, n = 4; p=0.046). The experimental results suggest a shift from I_f to Ca^{2+} dependent pacemaker mechanisms during β-adrenergic stimulation.

To rule out that loss of Pak1 interferes with atrial conduction and thereby impairs impulse propagation out of the sinus node, we recorded atrial conduction velocity using a MEA recording system. However, no difference in atrial conduction velocity that would be indicative of structural atrial remodeling (Supplemental Fig. 3) was determined.

3.4 Regulation of Pak1 dependent HCN4 activity

HCN4 is the major HCN isoform in the human and mouse SAN and its expression is regulated by the transcription factor myocyte enhancer factor-2 (MEF-2) [59,60]. MEF-2 activity is under the control of class II histone deacetylase 4 (HDAC4) where increased HDAC4 activity correlates with a suppressed MEF-2 dependent HCN4 expression [60]. To determine the role of class II HDACs in the attenuation of HCN4 activity, WT and Pak1$^{-/-}$ mice were treated with the class II HDAC inhibitor LMK235 (5 mg/kg/day for 3 days) [43]. At the end of LMK235 treatment the difference in basal HR was abrogated between male and female WT$_{LMK}$ and Pak1$^{-/-}{}_{LMK}$ hearts (Fig. 4Aa,Ba: WT$_{♂LMK}$: 322.4 ± 21.1 bpm, n = 5; Pak1$^{-/-}{}_{♂LMK}$: 314.5 ± 7.67 bpm, n= 5; $p = 0.984$; WT$_{♀LMK}$: 348.2 ± 44.5 bpm, n = 5; Pak1$^{-/-}{}_{♀LMK}$: 309.4 ± 58.0 bpm, n= 4; p = 0.552) and perfusion of the hearts with IVA revealed a significant increase in the contribution of I_f to pacemaker activity in Pak1$^{-/-}{}_{LMK}$ hearts (Fig. 4Ab,Bb: WT$_{♂LMK}$: −38.94 ± 18.56 %, n = 5; Pak1$^{-/-}{}_{♂LMK}$: −38.74 ± 2.51 %, n = 4; p > 0.999; WT$_{♀LMK}$: −39.94 ± 8.88 %, n = 4; Pak1$^{-/-}{}_{♀LMK}$: −45.68 ± 8.83 %, n= 4; p = 0.832). The contribution of the Ca^{2+} clock remained unaltered (Fig. 4 Ac,Bc: WT$_{♂LMK}$: −9.98 ± 8.20 %, n = 5; Pak1$^{-/-}{}_{♂LMK}$: −12.18 ± 4.57 %, n= 4; $p = 0.979$; WT$_{♀LMK}$: −15.58 ± 10.22 %, n = 3; Pak1$^{-/-}{}_{♀LMK}$: −9.06 ± 6.86 %, n= 4; $p = 0.607$). β-adrenergic stimulation of protein kinase A (PKA) leads to class II HDAC activation and MEF-2 suppression [61]. To rule out that the increased class II HDAC activity in Pak1$^{-/-}$ animals is due to the increased β-adrenergic tone, Pak1$^{-/-}$ animals were treated with the β-adrenergic receptor blocker atenolol (2.5 mg/kg, twice a day for 3 days) [45]. However, atenolol treatment did not alter the intrinsic HR nor the contribution of I_f or Ca^{2+} clock to pacemaker activity (Supplemental Fig. 4A–C) in Pak1$^{-/-}$ animals. The data suggest that loss of Pak1 increases class II HDAC activity and attenuates the contribution of HCN to pacemaker activity. Since in both sexes Pak1 altered SAN activity in a comparable manner and through the same

signaling mechanism, in further experiments we combined the data from both sexes when no statistical significance between males and females was identified.

3.5 Dependence of HCN activity on ROS

We previously demonstrated that the attenuation of Pak1 activity leads to increased NOX2 dependent production of ROS in atrial and ventricular myocytes [33,35]. To determine if an increased ROS production contributes to the altered pacemaker activity in $Pak1^{-/-}$ mice, animals were treated with the ROS scavenger TEMPOL (suppl. drinking water, 2 mmol/L for 2 days) [33,44]. TEMPOL treatment abrogated the difference in HR between $Pak1^{-/-}{}_{TEMP}$ and WT_{TEMP} (Fig. 5A: WT_{Temp}: 335.5 ± 23.86 bpm, n = 7; $Pak1^{-/-}{}_{Temp}$: 310.0 ± 42.8 bpm, n = 7; $p = 0.618$) and comparable to class II HDAC inhibition, IVA perfusion revealed a significant increase in the contribution of I_f to $Pak1^{-/-}$ pacemaker activity, making its contribution comparable to that in WT hearts (Fig. 5B: WT: −44.68 ± 7.15 %, n = 11; WT_{Temp}: −45.14 ± 8.03 %, n = 6; $p = 0.999$; $Pak1^{-/-}$: −20.66 ± 8.19 %, n = 12; $Pak1^{-/-}{}_{Temp}$: −39.51 ± 6. 28 %, n= 7; $p < 0.0001$). The contribution of the Ca^{2+} clock to pacemaker activity in $Pak1^{-/-}{}_{Temp}$ and WT_{Temp} hearts remained unchanged (Fig. 5C: WT: −21.87 ± 8.97 %, n = 9; WT_{Temp}: −16.57 ± 9.55 %, n = 6; p=0.577; $Pak1^{-/-}$: −20.17 ± 6.13 %, n = 9; $Pak1^{-/-}{}_{Temp}$: −14.02 ± 4.39 %, n = 4; $p = 0.564$). Inhibition of class I HDAC was linked to increased expression of free radical scavengers' catalase and super oxide dismutase whereas peroxiredoxins are direct targets of class IIb HDAC6 [62]. To determine if the class II HDAC inhibitor alters HCN activity by attenuating cellular oxidative stress in $Pak1^{-/-}$ animals we measured ROS production in isolated atrial myocytes from WT, $Pak1^{-/-}$ and $Pak1^{-/-}{}_{LMK}$ hearts. As previously reported, $Pak1^{-/-}$ atrial myocytes exhibited an increased ROS production compared to WT that remained increased in $Pak1^{-/-}{}_{LMK}$ atria (Fig. 5D). The data suggest that the increased ROS production in $Pak1^{-/-}$ animals attenuates the contribution of HCN to pacemaker activity and that class II HDAC activity does not alter, but rather is regulated downstream of the increased ROS production.

3.6 Mechanism of Pak1 dependent class II HDAC regulation

Activation of cardiac class II HDACs depends on their phosphorylation status. CaMKII dependent phosphorylation facilitates HDAC4 inactivation and export from the nucleus [63,64]. On the other hand, phosphorylation through PKA and ERK1/2 maintains HDAC4 activity and its localization inside the nucleus [61,65]. To determine if Pak1 regulates ERK1/2 activity we treated cultured atrial like myocytes (HL-1 cells) with Pak1-siRNA (48 h; Fig. 6Aa–c). Attenuation of Pak1 activity significantly increased ERK1/2 and p38 phosphorylation. To determine if increased ERK1/2 phosphorylation contributes to decreased pacemaker function in $Pak1^{-/-}$, WT and $Pak1^{-/-}$ mice were treated with the ERK1/2 inhibitor SCH772984 (ERK_i: 25 mg/kg, for 3 days). At the end of treatment, a difference in basal HR was no longer determined between WT_{ERKi} and $Pak1^{-/-}{}_{ERKi}$ hearts (Fig. 6B: WT_{ERKi}: 343.9 ± 22.5 bpm, n = 4; $Pak1^{-/-}{}_{ERKi}$: 325.3 ± 25.2 bpm, n = 5; p = 0.890) and perfusion of hearts with IVA revealed an increased contribution of I_f to pacemaker activity in $Pak1^{-/-}{}_{ERKi}$ (Fig. 6C: $Pak1^{-/-}$: −20.66 ± 8.19 %, n = 12; $Pak1^{-/-}{}_{ERKi}$: −36.88 ± 8.33 %, n = 5; p = 0.004). ERK1/2 inhibition had no effect on the Ca^{2+} clock mechanism.

3.7 Contribution of Pak1 regulation of HCN4 to atrial arrhythmic activity

We have previously demonstrated that loss of Pak1 activity increases the propensity for AF through enhanced NOX2 dependent ROS production [33,35]. To determine if in Pak1$^{-/-}$ animals SAN bradycardia contributes to the increased susceptibility for AF, the propensity for atrial arrhythmia was quantified in Langendorff perfused hearts using a burst pacing protocol [35]. As previously reported, under control conditions an increased number of Pak1$^{-/-}$ hearts exhibited pacing induced arrhythmia (Fig. 7AB) and individual Pak1$^{-/-}$ hearts presented with an augmented number of arrhythmic episodes (Fig. 7C). While treatment of Pak1$^{-/-}$ animals with the class II HDAC or ERK1/2 inhibitors increased the contribution of I_f to pacemaker activity, they did not rescue the increased propensity for AF in Pak1$^{-/-}$. TEMPOL treatment on the other hand as previously described, attenuated the number of Pak1$^{-/-}$ hearts with AF episodes as well as the number of AF episodes (Fig. 7B,C) thereby eliminating differences between WT and Pak1$^{-/-}$ animals. The data support that in Pak1$^{-/-}$ animals, rescuing the contribution of I_f to pacemaker activity alone, is insufficient to attenuate the increased risk for atrial arrhythmia.

4. Discussion

In the present study we demonstrate for the first time that in male and female hearts Pak1 plays an important role in maintaining the intrinsic SAN frequency by regulating HCN4 expression and the contribution of I_f to pacemaker activity. Pak1 activity attenuates ERK1/2 phosphorylation and thereby antagonizes the class II HDAC dependent suppression of MEF-2 and HCN4 expression.

4.1 Pak1

Pak1 is a serine/threonine kinase that is activated by the RAS-related G-proteins Rac1 and Cdc42. In the cardiac muscle Pak1 regulates contractility and excitability [66,67] and contributes to cardioprotective signaling [31,33,34]. Studies over the last years demonstrated that Pak1 signaling maintains the t-tubular structure and thereby the Ca^{2+} handling properties in ventricular myocytes, that loss of Pak1 increases the vulnerability for cardiac ischemia reperfusion injury and hypertrophic remodeling [31,32,34], and that Pak1$^{-/-}$ mice exhibit an increased propensity for atrial arrhythmia through spontaneous arrhythmic Ca^{2+} release events [35]. Pak1 has also been shown to modulate SAN frequency. Through its downstream target PP2A, it attenuates the activation of $Ca_v1.2$ and $K_v1.1$ (delayed rectifier potassium channel) during β-adrenergic stimulation [42] and altered Pak1 expression consequently changes the myocytes response to sympathetic agonists [68]. Stimulation of adenylate cyclase activity, despite the reduced contribution of I_f to pacemaker activity, increases SR to a larger degree in Pak1$^{-/-}$ than in WT hearts because of a relatively larger contribution of the Ca^{2+}-clock (Supplemental Fig. 2) likely driven by increased VDCC activity and load of the sarcoplasmic reticulum. Despite the regulatory role of Pak1 in the SAN, we and others have demonstrated that in awake and anesthetized Pak1$^{-/-}$ mice the basal HR is comparable to WT animals [35,42]. Here we demonstrate that this apparent lack of change is the consequence of an altered autonomic tone (Fig. 2AB). The increased β-adrenergic tone could be the consequence of the attenuated vagal tone in Pak1$^{-/-}$ animals [68] however, it does not contribute to the remodeling of the pacemaker rhythm

(Supplemental Fig. 4A–C). Given the unaltered $I_{K,ACh}$ activity and SAN responsiveness to CCh (Fig. 2CD) [55,56] the mechanism by which the vagal tone is attenuated in Pak1$^{-/-}$ animals remains to be determined. In contrast to male mice, we did not determine a significant difference in β-adrenergic tone between female WT and Pak1$^{-/-}$ mice. Given that the β-AR signaling does not influence the changes in SAN function, we did not further pursue this difference.

4.2 SAN Bradycardia

Cardiac excitation originates in specialized pacemaker cells within the SAN [1] that are under the continuous control of the sympathetic and parasympathetic branches of the ANS [47,69]. Our new data demonstrate SAN bradycardia in the hearts from Pak1$^{-/-}$ mice when ANS activity is suppressed. SAN bradycardia is a manifestation of SND which describes the inability of the heart's natural pacemaker to generate cardiac excitation in an appropriate frequency. SND can be the consequence of autonomic dysregulation, structural remodeling of the SAN, as well as genetic or post-translational modifications at the ion channel level [23,70,71]. In patients without cardiovascular diseases, SND is often linked to an ANS imbalance [72,73]. SAN bradycardia thereby can be the consequence of hypervagotonic signaling through the activation of $I_{K,ACh}$ or suppression of HCN4 activity [74,75]. In Pak1$^{-/-}$ hearts however, SAN bradycardia persisted in the isolated heart underlining its independence of ANS signaling.

4.3 SAN fibrosis

SAN bradycardia independent of ANS signaling, can be the consequence of tissue or ion channel remodeling. Increased SAN fibrosis can attenuate pacemaker function by increasing the capacitive load of the pacemaker cells [53] or by delaying and blocking the propagation of excitation out of the SAN [2,76] however, under control conditions no increase in cardiac fibrosis was determined in Pak1$^{-/-}$ animals [34]. Our data further show no delay in atrial conduction velocity that would be indicative of structural atrial remodeling (Supplemental Fig. 3) and the reversibility of the attenuated pacemaker activity would not support structural remodeling as a cause. Loss of Pak1 activity therefore is more likely to alter pacemaker activity on the cellular level.

4.4 Contribution of the Ca^{2+} and Membrane Clock to Pacemaker Activity

In GWAS studies SND has been linked to mutations in ion channels (SCN5A, HCN4, CaCNA1D) as well as Ca^{2+} handling proteins (RyR2, NCX, CASQ2) that play integral parts in the membrane and Ca^{2+} clock mechanism, respectively [4,70]. The Ca^{2+} clock is driven by sub-sarcolemmal Ca^{2+} release from RyR or IP_3R channels, which is translated into a depolarization of V_m through NCX dependent Ca^{2+} extrusion [11,13,15]. The initial increase in $[Ca^{2+}]_i$ is further amplified by the activation of T-type ($Ca_v3.1$) and L-type ($Ca_v1.3$ and then $Ca_v1.2$) Ca^{2+} channels that increase $[Ca^{2+}]_i$ through Ca^{2+} influx and Ca^{2+} induced Ca^{2+} release from RyR [13,27]. Previous analysis of the Ca^{2+} handling properties in atrial and ventricular myocytes, did not reveal a difference in VDCC, the CaT amplitude, and load of the sarcoplasmic reticulum between Pak1$^{-/-}$ and WT myocytes [31,33,35]. CPA suppressed pacemaker activity by about 21% which is lower that what was previously described in rabbit SAN cells. The decreased contribution of the Ca^{2+} clock could be species

dependent or due to an incomplete block of SERCA. However, when experiments were repeated in presence of caffeine (20 mmol/L) the results were comparable to those in the presence of CPA (Supplemental Fig. 1). Nevertheless, CPA and caffeine both failed to eliminate the difference in pacemaker activity between WT and Pak1$^{-/-}$ hearts (Fig. 3Ac) supporting that the contribution of the Ca^{2+} clock was not altered by loss of Pak1.

A prominent contributor to the membrane clock mechanism is the HCN channel that carries the pacemaker current (I_f) [18,19,21]. Loss of function mutations in HCN4 have been associated with SAN bradycardia and SND [18,20] as well as atrial fibrillation [21,22]. In Pak1$^{-/-}$ hearts IVA, a blocker of HCN channel isoforms, acutely eliminated the difference in HR between WT and Pak1$^{-/-}$ hearts supporting a Pak1 dependent alteration of this membrane clock mechanism.

The expression of HCN channels is regulated through the transcription factors TBX3 and ISL1, which control the SAN gene program and a transcription factor-binding site for MEF-2 has been identified within the HCN4 promoter region [59,60]. MEF-2 which regulates cardiomyocyte proliferation, apoptosis, and metabolism, can be activated through agonist stimulation (e.g., endothelin-1, sphingosine-1 phosphate, LPA) and in podocytes, direct phosphorylation was demonstrated through Pak1 dependent p38 stimulation [77]. We demonstrate increased p38 phosphorylation as a consequence of Pak1 inhibition (Fig. 6Ac) excluding this signaling pathway as a mechanism for attenuated MEF-2 dependent HCN expression in Pak1$^{-/-}$ hearts.

In the adult heart, MEF-2 activity is further regulated through its dimerization with class II HDACs [78]. Our experimental data show that class II HDAC inhibition does not affect pacemaker activity in WT hearts but rescues I_f activity in Pak1$^{-/-}$ animals supporting that under physiological conditions in the SAN, class II HDACs are in an inactive state and attenuation of Pak1 promotes their activation. HDAC activity is controlled by its phosphorylation status that modulates nuclear/cytoplasmic shuttling. CaMKII, PKD1, and AMPK are kinases that promote HDAC phosphorylation and nuclear export [63]. Nuclear import or activation on the other hand are enhanced by protein phosphatase 1 and PP2A dependent dephosphorylation [61,64], or PKA and ERK1/2 dependent phosphorylation [61,65]. While the β-adrenergic tone is increased (Fig. 2B) and β-adrenergic response is enhanced in Pak1$^{-/-}$ animals (Supplemental Fig. 2), the β-blocker atenolol did not rescue HCN4 activity in the SAN (Supplemental Fig. 4) ruling out increased PKA dependent signaling as a mechanism of HDAC activation. PP2A activity, that would favor the dephosphorylated state of HDAC and its nuclear localization, was described to be attenuated in Pak1$^{-/-}$ heart [34]. Attenuated PP2A activity thereby could overall increase HDAC phosphorylation making its activity dependent on kinase activity. We report an increase in the phosphorylation of the MAP kinase ERK1/2 during attenuated Pak1 activity (Fig. 6 Ab). A limitation of these data is that they were obtained in an atrial myocyte like cell line (HL-1) and not SAN cells however, given that ERK1/2 inhibition restores SAN function in Pak1$^{-/-}$ hearts, supports its involvement in HDAC activation.

HDAC4 activity has been described to depend on the cellular redox status. In the ventricular muscle the reduction of cysteine residues 667 and 669 in HDAC4 inhibited its nuclear export

independent of its phosphorylation status and prevented hypertrophic remodeling [79]. In the SAN on the other hand a reduction in cellular ROS through NOX2 inhibition or thioredoxin overexpression facilitated HDAC4s nuclear export and attenuated its activity [40]. The mechanism of this differential HDAC regulation in the ventricular muscle compared to the pacemaker and conduction system has not yet been determined. Our data are consistent with a ROS and ERK1/2 dependent increase of class II HDAC activity in the SAN. We cannot rule out that the redox state of class II HDACs is altered however, we propose that a ROS dependent increase in p-ERK1/2 in context with the attenuated PP2A activity promotes the HDAC4 mediated suppression of MEF-2 and thereby HCN expression.

4.5 Mechanism of Atrial Arrhythmia in Pak1$^{-/-}$ hearts

SAN bradycardia or SND increase the susceptibility for atrial arrhythmia by facilitating the occurrence of reentry and spontaneous arrhythmic events outside the SAN [3,4,6]. We have previously demonstrated that attenuated Pak1 activity increased NOX2 dependent ROS production that enhanced the occurrence of Ca^{2+} dependent arrhythmic events [33,35]. There is increasing evidence that HDAC activity can contribute to progressive atrial remodeling under conditions of AF [80]. Inhibition of class I HDACs, thereby reduced atrial dilatation and fibrosis, preserved atrial myocytes' ultrastructure, and delayed the onset of AF whereas class IIb HDAC6 activation induced contractile dysfunction and increased the risk for AF. In our hands the attenuation of class II HDAC and ERK1/2 activity as well as ROS scavenging restored the contribution of I_f to pacemaker activity. But only the suppression of ROS, as previously described, also reduced the increased propensity for atrial arrhythmia in Pak1$^{-/-}$ hearts. While we have not quantified the activity of class II HDAC and class II HDAC dependent changes in atrial protein expression at this point its contribution to atrial arrhythmia does not seem to be significant in our model.

5. Limitations

In our experimental approach we have not further quantified the current densities and kinetics of I_f, VDCCs [13,27–29], $I_{Na,TTX}$ [24,25], TRPM and TRPC channels [26] by voltage clamp recordings. Accordingly, we can't entirely rule out that differences in these parameters, especially the current kinetic, exist. However, we would expect these differences to be minor given that a) the difference in pacemaker activity was eliminated by IVA, b) the difference in I_f contribution can be explained by reduced HCN4 protein expression in Pak1$^{-/-}$ myocyte, and c) CPA and caffeine experiments support a comparable contribution of the Ca^{2+} stores to pacemaker activity in WT and Pak1$^{-/-}$ mice. Even though we did not isolate the contribution of Ca^{2+} influx, the fact that the load of the sarcoplasmic reticulum was unchanged (Supplemental Fig.1) which closely depends on Ca^{2+} influx, suggests that potential changes in Ca^{2+} influx amplitude or kinetic were not relevant to the described differences in Pak1$^{-/-}$ HR [31,33,35,42]. We also did not further detail potential changes in the activity of Phophodiesterases (PDE) that regulate the myocytes response to β-adrenergic stimulation. To explain the increased β-adrenergic tone in vivo, an attenuated PDE activity could be assumed; however, this would be inconsistent with the attenuated contribution of I_f to pacemaker activity. An increased PDE activity on the other hand, would be expected to attenuate I_f but under these conditions, also a decreased response to β-adrenergic stimulation

or activation of VDCC and the Ca^{2+} clock would be assumed. Since neither case is supported by our experimental results, we did not further pursue this line of investigation.

6. Conclusion

Our results demonstrate that Pak regulates intrinsic pacemaker activity by maintaining HCN expression. Attenuation of Pak1 enhances NOX2 dependent ROS production and increases ERK1/2 activity, which results in enhanced class II HDAC activity and a decrease in I_f. We demonstrated that in $Pak1^{-/-}$ hearts, attenuation of ROS but not attenuation of SAN bradycardia is protective against AF. Our results establish Pak1 as a class II HDAC regulator and potential therapeutic target for SAN dysfunction.

Supplementary Material

Refer to Web version on PubMed Central for supplementary material.

Acknowledgements:

This work was supported by funding from the National Institutes for Health R01s to KB (HL128330, HL155762, and HL164453).

Data availability statement

The data that support the findings of this study are available from the corresponding author upon reasonable request.

Abbreviations:

AC	adenylate cyclase
ANS	autonomic nervous system
APs	action potentials
AF	atrial fibrillation
Ca^{2+}	calcium
caff	caffeine
CaMKII	Ca^{2+} calmodulin kinase II
CCh	carbachol
DCF	2′,7′-dichlorofluorescein diacetate
HDAC	histone deacetylase
HCN	cyclic-nucleotide gated cation channel
CPA	cyclopiazonic acid
ECG	Electrocardiogram

ERK1/2	Extracellular Signal-Regulated Kinase 1/2
GIRK	G-protein activated inwardly rectifying K-channel
HR	heart rate
IP_3R	inositol 1,4,5-tris phosphate receptor
IP	intraperitoneal
IVA	ivabradine
MEA	multielectrode array
Na^+	sodium
NADPH	nicotinamide adenine dinucleotide phosphate
NOX2	NADPH oxidase 2
MAPK	mitogen-activated protein kinase
V_m	membrane potential
MEF-2	myocyte enhancer factor-2
Pak1	p21-activated kinase 1
$Pak1^{-/-}$	Pak1 deficient mice
PP2A	protein phosphatase 2A
PKA	protein kinase A
ROS	reactive oxygen species
RyR	ryanodine receptor
SAN	sinoatrial node
SERCA	sarco/endoplasmic reticulum Ca^{2+}-ATPase
SR	sinus rhythm
SND	sinus node dysfunction
NCX	sodium calcium exchanger
TerQ	tertiapin-q
VDCC	voltage dependent Calcium channels
WT	wildtype

References

[1]. Choudhury M, Boyett MR, Morris GM, Biology of the Sinus Node and its Disease, Arrhythmia Electrophysiol Rev. 4 (2015) 28–34. 10.15420/aer.2015.4.1.28.

[2]. Egom EE, Vella K, Hua R, Jansen HJ, Moghtadaei M, Polina I, Bogachev O, Hurnik R, Mackasey M, Rafferty S, Ray G, Rose RA, Impaired sinoatrial node function and increased susceptibility to atrial fibrillation in mice lacking natriuretic peptide receptor C., J. Physiol. (Lond.). 593 (2015) 1127–1146. 10.1113/jphysiol.2014.283135. [PubMed: 25641115]

[3]. Yang P-S, Kim D, Jang E, Yu HT, Kim T-H, Sung J-H, Pak H-N, Lee M-H, Joung B, Risk of sick sinus syndrome in patients diagnosed with atrial fibrillation: A population-based cohort., J Cardiovasc Electr. 32 (2021) 2704–2714. 10.1111/jce.15202.

[4]. DiFrancesco D, HCN4, Sinus Bradycardia and Atrial Fibrillation., Arrhythmia Electrophysiol Rev. 4 (2015) 9–13. 10.15420/aer.2015.4.1.9.

[5]. Elvan A, Wylie K, Zipes DP, Pacing-induced chronic atrial fibrillation impairs sinus node function in dogs. Electrophysiological remodeling., Circulation. 94 (1996) 2953–60. 10.1161/01.cir.94.11.2953. [PubMed: 8941126]

[6]. Kim JJ, Němec J, Papp R, Strongin R, Abramson JJ, Salama G, Bradycardia alters Ca2+ dynamics enhancing dispersion of repolarization and arrhythmia risk, Am J Physiol-Heart C. 304 (2013) H848–H860. 10.1152/ajpheart.00787.2012.

[7]. Manios EG, Kanoupakis EM, Mavrakis HE, Kallergis EM, Dermitzaki DN, Vardas PE, Sinus Pacemaker Function after Cardioversion of Chronic Atrial Fibrillation: Is Sinus Node Remodeling Related with Recurrence?, J Cardiovasc Electr. 12 (2001) 800–806. 10.1046/j.1540-8167.2001.00800.x.

[8]. Yeh Y-H, Burstein B, Qi XY, Sakabe M, Chartier D, Comtois P, Wang Z, Kuo C-T, Nattel S, Funny current downregulation and sinus node dysfunction associated with atrial tachyarrhythmia: a molecular basis for tachycardia-bradycardia syndrome., Circulation. 119 (2009) 1576–1585. 10.1161/circulationaha.108.789677. [PubMed: 19289641]

[9]. Gao Z, Chen B, Joiner ML, Wu Y, Guan X, Koval OM, Chaudhary AK, Cunha SR, Mohler PJ, Martins JB, Song LS, Anderson ME, I(f) and SR Ca(2+) release both contribute to pacemaker activity in canine sinoatrial node cells, J. Mol. Cell. Cardiol. 49 (2010) 33–40. http://www.ncbi.nlm.nih.gov/entrez/query.fcgi?cmd=Retrieve&;db=PubMed&dopt=Citation&list_uids=20380837. [PubMed: 20380837]

[10]. Maltsev VA, Lakatta EG, Dynamic interactions of an intracellular Ca2+ clock and membrane ion channel clock underlie robust initiation and regulation of cardiac pacemaker function, Cardiovasc. Res. 77 (2008) 274–284. http://www.ncbi.nlm.nih.gov/entrez/query.fcgi?cmd=Retrieve&;db=PubMed&dopt=Citation&list_uids=18006441. [PubMed: 18006441]

[11]. Kapur N, Banach K, Inositol-1,4,5-trisphosphate-mediated spontaneous activity in mouse embryonic stem cell-derived cardiomyocytes., J. Physiol. (Lond.). 581 (2007) 1113–1127. 10.1113/jphysiol.2006.125955. [PubMed: 17379641]

[12]. Vinogradova TM, Zhou Y-Y, Maltsev V, Lyashkov A, Stern M, Lakatta EG, Rhythmic ryanodine receptor Ca2+ releases during diastolic depolarization of sinoatrial pacemaker cells do not require membrane depolarization., Circ Res. 94 (2004) 802–809. 10.1161/01.res.0000122045.55331.0f. [PubMed: 14963011]

[13]. Huser J, Blatter LA, Lipsius SL, Intracellular Ca2+ release contributes to automaticity in cat atrial pacemaker cells., J. Physiol. (Lond.). 524 Pt 2 (2000) 415–422. http://eutils.ncbi.nlm.nih.gov/entrez/eutils/elink.fcgi?dbfrom=pubmed&;id=10766922&retmode=ref&cmd=prlinks. [PubMed: 10766922]

[14]. Vinogradova TM, Zhou YY, Maltsev V, Lyashkov A, Stern M, Lakatta EG, Rhythmic ryanodine receptor Ca2+ releases during diastolic depolarization of sinoatrial pacemaker cells do not require membrane depolarization, Circ Res. 94 (2004) 802. [PubMed: 14963011]

[15]. Bogdanov KY, Vinogradova TM, Lakatta EG, Sinoatrial nodal cell ryanodine receptor and Na(+)-Ca(2+) exchanger: molecular partners in pacemaker regulation, Circ Res. 88 (2001) 1254–1258. [PubMed: 11420301]

[16]. Vinogradova TM, Brochet DXP, Sirenko S, Li Y, Spurgeon H, Lakatta EG, Sarcoplasmic Reticulum Ca2+ Pumping Kinetics Regulates Timing of Local Ca2+ Releases and Spontaneous Beating Rate of Rabbit Sinoatrial Node Pacemaker Cells, Circ Res. 107 (2010) 767–775. 10.1161/circresaha.110.220517. [PubMed: 20651285]

[17]. Stieber J, Herrmann S, Feil S, Loster J, Feil R, Biel M, Hofmann F, Ludwig A, The hyperpolarization-activated channel HCN4 is required for the generation of pacemaker action potentials in the embryonic heart, Proc. Natl. Acad. Sci. U.S.A. 100 (2003) 15235–15240. http://www.ncbi.nlm.nih.gov/entrez/query.fcgi?cmd=Retrieve&;db=PubMed&dopt=Citation&list_uids=14657344. [PubMed: 14657344]

[18]. Nof E, Luria D, Brass D, Marek D, Lahat H, Reznik-Wolf H, Pras E, Dascal N, Eldar M, Glikson M, Point Mutation in the HCN4 Cardiac Ion Channel Pore Affecting Synthesis, Trafficking, and Functional Expression Is Associated With Familial Asymptomatic Sinus Bradycardia, Circulation. 116 (2007) 463–470. 10.1161/circulationaha.107.706887. [PubMed: 17646576]

[19]. Accili EA, Proenza C, Baruscotti M, DiFrancesco D, From funny current to HCN channels: 20 years of excitation, News Physiol Sci. 17 (2002) 32–37. [PubMed: 11821534]

[20]. Milano A, Vermeer AMC, Lodder EM, Barc J, Verkerk AO, Postma AV, van der Bilt IAC, Baars MJH, van Haelst PL, Caliskan K, Hoedemaekers YM, Scouarnec SL, Redon R, Pinto YM, Christiaans I, Wilde AA, Bezzina CR, HCN4 Mutations in Multiple Families With Bradycardia and Left Ventricular Noncompaction Cardiomyopathy, J Am Coll Cardiol. 64 (2014) 745–756. 10.1016/j.jacc.2014.05.045. [PubMed: 25145517]

[21]. Baruscotti M, Bucchi A, Viscomi C, Mandelli G, Consalez G, Gnecchi-Rusconi T, Montano N, Casali KR, Micheloni S, Barbuti A, DiFrancesco D, Deep bradycardia and heart block caused by inducible cardiac-specific knockout of the pacemaker channel gene Hcn4, Proc National Acad Sci. 108 (2011) 1705–1710. 10.1073/pnas.1010122108.

[22]. Macri V, Mahida SN, Zhang ML, Sinner MF, Dolmatova EV, Tucker NR, McLellan M, Shea MA, Milan DJ, Lunetta KL, Benjamin EJ, Ellinor PT, A novel trafficking-defective HCN4 mutation is associated with early-onset atrial fibrillation, Heart Rhythm. 11 (2014) 1055–1062. 10.1016/j.hrthm.2014.03.002. [PubMed: 24607718]

[23]. Ishikawa T, Ohno S, Murakami T, Yoshida K, Mishima H, Fukuoka T, Kimoto H, Sakamoto R, Ohkusa T, Aiba T, Nogami A, Sumitomo N, Shimizu W, Yoshiura K, Horigome H, Horie M, Makita N, Sick sinus syndrome with HCN4 mutations shows early onset and frequent association with atrial fibrillation and left ventricular noncompaction, Heart Rhythm. 14 (2017) 717–724. 10.1016/j.hrthm.2017.01.020. [PubMed: 28104484]

[24]. Lei M, Goddard C, Liu J, Leoni AL, Royer A, Fung SS, Xiao G, Ma A, Zhang H, Charpentier F, Vandenberg JI, Colledge WH, Grace AA, Huang CL, Sinus node dysfunction following targeted disruption of the murine cardiac sodium channel gene Scn5a, J Physiol. 567 (2005) 387–400. http://www.ncbi.nlm.nih.gov/entrez/query.fcgi?cmd=Retrieve&;db=PubMed&dopt=Citation&list_uids=15932895. [PubMed: 15932895]

[25]. Lei M, Jones SA, Liu J, Lancaster MK, Fung SS-M, Dobrzynski H, Camelliti P, Maier SKG, Noble D, Boyett MR, Requirement of neuronal- and cardiac-type sodium channels for murine sinoatrial node pacemaking, J Physiology. 559 (2004) 835–848. 10.1113/jphysiol.2004.068643.

[26]. Demion M, Bois P, Launay P, Guinamard R, TRPM4, a Ca2+-activated nonselective cation channel in mouse sino-atrial node cells., Cardiovasc. Res. 73 (2007) 531–538. 10.1016/j.cardiores.2006.11.023. [PubMed: 17188667]

[27]. Mangoni ME, Traboulsie A, Leoni AL, Couette B, Marger L, Quang KL, Kupfer E, Cohen-Solal A, Vilar J, Shin HS, Escande D, Charpentier F, Nargeot J, Lory P, Bradycardia and slowing of the atrioventricular conduction in mice lacking CaV3.1/alpha1G T-type calcium channels, Circ Res. 98 (2006) 1422–1430. http://www.ncbi.nlm.nih.gov/entrez/query.fcgi?cmd=Retrieve&;db=PubMed&dopt=Citation&list_uids=16690884. [PubMed: 16690884]

[28]. Toyoda F, Mesirca P, Dubel S, Ding W-G, Striessnig J, Mangoni ME, Matsuura H, CaV1.3 L-type Ca2+ channel contributes to the heartbeat by generating a dihydropyridine-sensitive persistent Na+ current, Sci Rep-Uk. 7 (2017) 7869. 10.1038/s41598-017-08191-8.

[29]. Torrente AG, Mesirca P, Neco P, Rizzetto R, Dubel S, Barrere C, Sinegger-Brauns M, Striessnig J, Richard S, Nargeot J, Gomez AM, Mangoni ME, L-type Cav1.3 channels regulate ryanodine

receptor-dependent Ca2+ release during sino-atrial node pacemaker activity, Cardiovasc Res. 109 (2016) 451–461. 10.1093/cvr/cvw006. [PubMed: 26786159]

[30]. Egom EEA, Ke Y, Musa H, Mohamed TMA, Wang T, Cartwright E, Solaro RJ, Lei M, FTY720 prevents ischemia/reperfusion injury-associated arrhythmias in an ex vivo rat heart model via activation of Pak1/Akt signaling., J. Mol. Cell. Cardiol. 48 (2010) 406–414. 10.1016/j.yjmcc.2009.10.009. [PubMed: 19852968]

[31]. Desantiago J, Bare DJ, Ke Y, Sheehan KA, Solaro RJ, Banach K, Functional integrity of the T-tubular system in cardiomyocytes depends on p21-activated kinase 1., J. Mol. Cell. Cardiol. 60 (2013) 121–128. 10.1016/j.yjmcc.2013.04.014. [PubMed: 23612118]

[32]. Monasky MM, Taglieri DM, Patel BG, Chernoff J, Wolska BM, Ke Y, Solaro RJ, P21-Activated Kinase Improves Cardiac Contractility during Ischemia-Reperfusion concomitant with changes in Troponin-T and Myosin Light Chain 2 Phosphorylation, Am. J. Physiol. Heart Circ. Physiol. 302 (2011) H224–H230. 10.1152/ajpheart.00612.2011. [PubMed: 22037191]

[33]. Desantiago J, Bare DJ, Xiao L, Ke Y, Solaro RJ, Banach K, p21-Activated kinase1 (Pak1) is a negative regulator of NADPH-oxidase 2 in ventricular myocytes., J. Mol. Cell. Cardiol. 67 (2014) 77–85. 10.1016/j.yjmcc.2013.12.017. [PubMed: 24380729]

[34]. Liu W, Zi M, Naumann R, Ulm S, Jin J, Taglieri DM, Prehar S, Gui J, Tsui H, Xiao R-P, Neyses L, Solaro RJ, Ke Y, Cartwright EJ, Lei M, Wang X, Pak1 as a novel therapeutic target for antihypertrophic treatment in the heart., Circulation. 124 (2011) 2702–2715. 10.1161/circulationaha.111.048785. [PubMed: 22082674]

[35]. Desantiago J, Bare DJ, Varma D, Solaro RJ, Arora R, Banach K, Loss of p21-activated kinase 1 (Pak1) promotes atrial arrhythmic activity., Heart Rhythm. 15 (2018) 1233–1241. 10.1016/j.hrthm.2018.03.041. [PubMed: 29625277]

[36]. Zhang H, Hao M, Li L, Chen K, Qi J, Chen W, Cai X, Chen C, Liu Z, Hou P, Shenxian-Shengmai Oral Liquid Improves Sinoatrial Node Dysfunction through the PKC/NOX-2 Signaling Pathway, Evidence-Based Complementary Altern Medicine Ecam. 2021 (2021) 5572140. 10.1155/2021/5572140.

[37]. Swaminathan PD, Purohit A, Soni S, Voigt N, Singh MV, Glukhov AV, Gao Z, He BJ, Luczak ED, Joiner MA, Kutschke W, Yang J, Donahue JK, Weiss RM, Grumbach IM, Ogawa M, Chen P-S, Efimov I, Dobrev D, Mohler PJ, Hund TJ, Anderson ME, Oxidized CaMKII causes cardiac sinus node dysfunction in mice., J Clin Investigation. 121 (2011) 3277–3288. 10.1172/jci57833.

[38]. Kondo H, Kira S, Oniki T, Gotoh K, Fukui A, Abe I, Ikebe Y, Kawano K, Saito S, Aoki K, Okada N, Nagano Y, Akioka H, Shinohara T, Akiyoshi K, Masaki T, Teshima Y, Yufu K, Nakagawa M, Takahashi N, Interleukin-10 treatment attenuates sinus node dysfunction caused by streptozotocin-induced hyperglycemia in mice, Cardiovasc Res. 115 (2018) 57–70. 10.1093/cvr/cvy162.

[39]. Chang X, Yao S, Wu Q, Wang Y, Liu J, Liu R, Tongyang Huoxue Decoction (TYHX) Ameliorating Hypoxia/Reoxygenation-Induced Disequilibrium of Calcium Homeostasis and Redox Imbalance via Regulating Mitochondrial Quality Control in Sinoatrial Node Cells, Oxid Med Cell Longev. 2021 (2021) 3154501. 10.1155/2021/3154501. [PubMed: 34422207]

[40]. Yang B, Huang Y, Zhang H, Huang Y, Zhou HJ, Young L, Xiao H, Min W, Mitochondrial thioredoxin-2 maintains HCN4 expression and prevents oxidative stress-mediated sick sinus syndrome., J. Mol. Cell. Cardiol. 138 (2020) 291–303. 10.1016/j.yjmcc.2019.10.009. [PubMed: 31751569]

[41]. Xue J-B, Val-Blasco A, Davoodi M, Gómez S, Yaniv Y, Benitah J-P, Gómez AM, Heart failure in mice induces a dysfunction of the sinus node associated with reduced CaMKII signaling, J Gen Physiol. 154 (2022) e202112895. 10.1085/jgp.202112895. [PubMed: 35452507]

[42]. Ke Y, Lei M, Collins TP, Rakovic S, Mattick PA, Yamasaki M, Brodie MS, Terrar DA, Solaro RJ, Regulation of L-type calcium channel and delayed rectifier potassium channel activity by p21-activated kinase-1 in guinea pig sinoatrial node pacemaker cells, Circ Res. 100 (2007) 1317–1327. http://www.ncbi.nlm.nih.gov/entrez/query.fcgi?cmd=Retrieve&;db=PubMed&dopt=Citation&list_uids=17413045. [PubMed: 17413045]

[43]. Choi SY, Kee HJ, Sun S, Seok YM, Ryu Y, Kim GR, Kee S, Pflieger M, Kurz T, Kassack MU, Jeong MH, Histone deacetylase inhibitor LMK235 attenuates vascular constriction and

aortic remodelling in hypertension, J Cell Mol Med. 23 (2019) 2801–2812. 10.1111/jcmm.14188. [PubMed: 30734467]

[44]. Sovari AA, Rutledge CA, Jeong E-M, Dolmatova E, Arasu D, Liu H, Vahdani N, Gu L, Zandieh S, Xiao L, Bonini MG, Duffy HS, Dudley SC, Mitochondria Oxidative Stress, Connexin43 Remodeling, and Sudden Arrhythmic Death., Circ Arrhythm Electrophysiol. 3 (2013) 623–631. 10.1161/circep.112.976787.

[45]. Sterin-Borda L, Gorelik G, Postan M, Cappa SG, Borda E, Alterations in cardiac beta-adrenergic receptors in chagasic mice and their association with circulating beta-adrenoceptor-related autoantibodies, Cardiovasc Res. 41 (1999) 116–125. 10.1016/s0008-6363(98)00225-9. [PubMed: 10325959]

[46]. Hayes TK, Neel NF, Hu C, Gautam P, Chenard M, Long B, Aziz M, Kassner M, Bryant KL, Pierobon M, Marayati R, Kher S, George SD, Xu M, Wang-Gillam A, Samatar AA, Maitra A, Wennerberg K, Petricoin EF, Yin HH, Nelkin B, Cox AD, Yeh JJ, Der CJ, Long-Term ERK Inhibition in KRAS-Mutant Pancreatic Cancer Is Associated with MYC Degradation and Senescence-like Growth Suppression, Cancer Cell. 29 (2016) 75–89. 10.1016/j.ccell.2015.11.011. [PubMed: 26725216]

[47]. Black N, D'Souza A, Wang Y, Piggins H, Dobrzynski H, Morris G, Boyett MR, Circadian rhythm of cardiac electrophysiology, arrhythmogenesis, and the underlying mechanisms., Heart Rhythm. 16 (2019) 298–307. 10.1016/j.hrthm.2018.08.026. [PubMed: 30170229]

[48]. Yaniv Y, Sirenko S, Ziman BD, Spurgeon HA, Maltsev VA, Lakatta EG, New evidence for coupled clock regulation of the normal automaticity of sinoatrial nodal pacemaker cells: Bradycardic effects of ivabradine are linked to suppression of intracellular Ca(2+) cycling., J. Mol. Cell. Cardiol. 62 (2013) 80–89. 10.1016/j.yjmcc.2013.04.026. [PubMed: 23651631]

[49]. Han SY, Bolter CP, Effects of tertiapin-Q and ZD7288 on changes in sinoatrial pacemaker rhythm during vagal stimulation, Autonomic Neurosci. 193 (2015) 117–126. 10.1016/j.autneu.2015.10.002.

[50]. Mabe AM, Hoover DB, Structural and functional cardiac cholinergic deficits in adult neurturin knockout mice., Cardiovasc. Res. 82 (2009) 93–99. 10.1093/cvr/cvp029. [PubMed: 19176599]

[51]. Varma D, Almeida JFQ, DeSantiago J, Blatter LA, Banach K, Inositol 1,4,5-trisphosphate receptor - reactive oxygen signaling domain regulates excitation-contraction coupling in atrial myocytes, J Mol Cell Cardiol. 163 (2022) 147–155. 10.1016/j.yjmcc.2021.10.006. [PubMed: 34755642]

[52]. Fahrenbach JP, Ai X, Banach K, Decreased intercellular coupling improves the function of cardiac pacemakers derived from mouse embryonic stem cells., J. Mol. Cell. Cardiol. 45 (2008) 642–649. 10.1016/j.yjmcc.2008.08.013. [PubMed: 18817780]

[53]. Fahrenbach JP, Mejia-Alvarez R, Banach K, The relevance of non-excitable cells for cardiac pacemaker function., J. Physiol. (Lond.). 585 (2007) 565–578. 10.1113/jphysiol.2007.144121. [PubMed: 17932143]

[54]. Mureli S, Gans CP, Bare DJ, Geenen DL, Kumar NM, Banach K, Mesenchymal stem cells improve cardiac conduction by upregulation of connexin 43 through paracrine signaling., Am. J. Physiol. Heart Circ. Physiol. 304 (2013) H600–H609. 10.1152/ajpheart.00533.2012. [PubMed: 23241322]

[55]. Dobrev D, Friedrich A, Voigt N, Jost N, Wettwer E, Christ T, Knaut M, Ravens U, The G protein-gated potassium current I(K,ACh) is constitutively active in patients with chronic atrial fibrillation, Circulation. 112 (2005) 3697–3706. [PubMed: 16330682]

[56]. Dobrev D, Graf E, Wettwer E, Himmel HM, Hala O, Doerfel C, Christ T, Schuler S, Ravens U, Molecular basis of downregulation of G-protein-coupled inward rectifying K(+) current (I(K,ACh) in chronic human atrial fibrillation: decrease in GIRK4 mRNA correlates with reduced I(K,ACh) and muscarinic receptor-mediated shortening of action potentials., Circulation. 104 (2001) 2551–2557. http://www.ncbi.nlm.nih.gov/entrez/query.fcgi?cmd=Retrieve&;db=PubMed&dopt=Citation&list_uids=11714649. [PubMed: 11714649]

[57]. Baudot M, Torre E, Bidaud I, Louradour J, Torrente AG, Fossier L, Talssi L, Nargeot J, Barrère-Lemaire S, Mesirca P, Mangoni ME, Concomitant genetic ablation of L-type Cav1.3 (α1D) and T-type Cav3.1 (α1G) Ca2+ channels disrupts heart automaticity, Sci Rep-Uk. 10 (2020) 18906. 10.1038/s41598-020-76049-7.

[58]. Valverde CA, Kornyeyev D, Ferreiro M, Petrosky AD, Mattiazzi A, Escobar AL, Transient Ca2+ depletion of the sarcoplasmic reticulum at the onset of reperfusion, Cardiovasc. Res. 85 (2010) 671–680. http://www.ncbi.nlm.nih.gov/entrez/query.fcgi?cmd=Retrieve&;db=PubMed&dopt=Citation&list_uids=19920131. [PubMed: 19920131]

[59]. Kuratomi S, Ohmori Y, Ito M, Shimazaki K, Muramatsu S-I, Mizukami H, Uosaki H, Yamashita JK, Arai Y, Kuwahara K, Takano M, The cardiac pacemaker-specific channel Hcn4 is a direct transcriptional target of MEF2., Cardiovasc. Res. 83 (2009) 682–687. 10.1093/cvr/cvp171. [PubMed: 19477969]

[60]. Vedantham V, Evangelista M, Huang Y, Srivastava D, Spatiotemporal regulation of an Hcn4 enhancer defines a role for Mef2c and HDACs in cardiac electrical patterning, Dev Biol. 373 (2013) 149–162. 10.1016/j.ydbio.2012.10.017. [PubMed: 23085412]

[61]. Backs J, Worst BC, Lehmann LH, Patrick DM, Jebessa Z, Kreusser MM, Sun Q, Chen L, Heft C, Katus HA, Olson EN, Selective repression of MEF2 activity by PKA-dependent proteolysis of HDAC4, J Cell Biol. 195 (2011) 403–415. 10.1083/jcb.201105063. [PubMed: 22042619]

[62]. Parmigiani RB, Xu WS, Venta-Perez G, Erdjument-Bromage H, Yaneva M, Tempst P, Marks PA, HDAC6 is a specific deacetylase of peroxiredoxins and is involved in redox regulation, Proc National Acad Sci. 105 (2008) 9633–9638. 10.1073/pnas.0803749105.

[63]. Gillette TG, HDAC Inhibition in the Heart, Circulation. 143 (2021) 1891–1893. 10.1161/circulationaha.121.054262. [PubMed: 33970677]

[64]. Veloso A, Martin M, Bruyr J, O'Grady T, Deroanne C, Mottet D, Twizere J-C, Cherrier T, Dequiedt F, Dephosphorylation of HDAC4 by PP2A-Bδ unravels a new role for the HDAC4/MEF2 axis in myoblast fusion, Cell Death Dis. 10 (2019) 512. 10.1038/s41419-019-1743-6. [PubMed: 31273193]

[65]. Zhou X, Richon VM, Wang AH, Yang X-J, Rifkind RA, Marks PA, Histone deacetylase 4 associates with extracellular signal-regulated kinases 1 and 2, and its cellular localization is regulated by oncogenic Ras, Proc National Acad Sci. 97 (2000) 14329–14333. 10.1073/pnas.250494697.

[66]. Ke Y, Wang L, Pyle WG, de Tombe PP, Solaro RJ, Intracellular localization and functional effects of P21-activated kinase-1 (Pak1) in cardiac myocytes, Circ Res. 94 (2004) 194–200. 10.1161/01.res.0000111522.02730.56. [PubMed: 14670848]

[67]. Sheehan KA, Ke Y, Solaro RJ, p21-Activated kinase-1 and its role in integrated regulation of cardiac contractility, Am. J. Physiol. Regul. Integr. Comp. Physiol. 293 (2007) R963–73. http://www.ncbi.nlm.nih.gov/entrez/query.fcgi?cmd=Retrieve&;db=PubMed&dopt=Citation&list_uids=17609315. [PubMed: 17609315]

[68]. Sheehan KA, Ke Y, Wolska BM, Solaro RJ, Expression of active p21-activated kinase-1 induces Ca2+ flux modification with altered regulatory protein phosphorylation in cardiac myocytes., Am. J. Physiol., Cell Physiol. 296 (2009) C47–58. 10.1152/ajpcell.00012.2008. [PubMed: 18923061]

[69]. MacDonald EA, Rose RA, Quinn TA, Neurohumoral Control of Sinoatrial Node Activity and Heart Rate: Insight From Experimental Models and Findings From Humans, Front Physiol. 11 (2020) 170. 10.3389/fphys.2020.00170. [PubMed: 32194439]

[70]. den Hoed M, Eijgelsheim M, Esko T, Brundel BJJM, Peal DS, Evans DM, Nolte IM, Segrè AV, Holm H, Handsaker RE, Westra H-J, Johnson T, Isaacs A, Yang J, Lundby A, Zhao JH, Kim YJ, Go MJ, Almgren P, Bochud M, Boucher G, Cornelis MC, Gudbjartsson D, Hadley D, van der Harst P, Hayward C, den Heijer M, Igl W, Jackson AU, Kutalik Z, Luan J, Kemp JP, Kristiansson K, Ladenvall C, Lorentzon M, Montasser ME, Njajou OT, O'Reilly PF, Padmanabhan S, Pourcain BS, Rankinen T, Salo P, Tanaka T, Timpson NJ, Vitart V, Waite L, Wheeler W, Zhang W, Draisma HHM, Feitosa MF, Kerr KF, Lind PA, Mihailov E, Onland-Moret NC, Song C, Weedon MN, Xie W, Yengo L, Absher D, Albert CM, Alonso A, Arking DE, de Bakker PIW, Balkau B, Barlassina C, Benaglio P, Bis JC, Bouatia-Naji N, Brage S, Chanock SJ, Chines PS, Chung M, Darbar D, Dina C, Dörr M, Elliott P, Felix SB, Fischer K, Fuchsberger C, de Geus EJC, Goyette P, Gudnason V, Harris TB, Hartikainen A-L, Havulinna AS, Heckbert SR, Hicks AA, Hofman A, Holewijn S, Hoogstra-Berends F, Hottenga J-J, Jensen MK, Johansson A, Junttila J, Kääb S, Kanon B, Ketkar S, Khaw K-T, Knowles JW, Kooner AS, Kors JA, Kumari M, Milani L, Laiho P, Lakatta EG, Langenberg C, Leusink M, Liu Y, Luben RN, Lunetta KL, Lynch

SN, Markus MRP, Marques-Vidal P, Leach IM, McArdle WL, McCarroll SA, Medland SE, Miller KA, Montgomery GW, Morrison AC, Müller-Nurasyid M, Navarro P, Nelis M, O'Connell JR, O'Donnell CJ, Ong KK, Newman AB, Peters A, Polasek O, Pouta A, Pramstaller PP, Psaty BM, Rao DC, Ring SM, Rossin EJ, Rudan D, Sanna S, Scott RA, Sehmi JS, Sharp S, Shin JT, Singleton AB, Smith AV, Soranzo N, Spector TD, Stewart C, Stringham HM, Tarasov KV, Uitterlinden AG, Vandenput L, Hwang S-J, Whitfield JB, Wijmenga C, Wild SH, Willemsen G, Wilson JF, Witteman JCM, Wong A, Wong Q, Jamshidi Y, Zitting P, Boer JMA, Boomsma DI, Borecki IB, van Duijn CM, Ekelund U, Forouhi NG, Froguel P, Hingorani A, Ingelsson E, Kivimäki M, Kronmal RA, Kuh D, Lind L, Martin NG, Oostra BA, Pedersen NL, Quertermous T, Rotter JI, van der Schouw YT, Verschuren WMM, Walker M, Albanes D, Arnar DO, Assimes TL, Bandinelli S, Boehnke M, de Boer RA, Bouchard C, Caulfield WLM, Chambers JC, Curhan G, Cusi D, Eriksson J, Ferrucci L, Gilst WHV, Glorioso N, de Graaf J, Groop L, Gyllensten U, Hsueh W-C, Hu FB, Huikuri HV, Hunter DJ, Iribarren C, Isomaa B, Järvelin M-R, Jula A, Kähönen M, Kiemeney LA, van der Klauw MM, Kooner JS, Kraft P, Iacoviello L, Lehtimäki T, Lokki M-LL, Mitchell BD, Navis G, Nieminen MS, Ohlsson C, Poulter NR, Qi L, Raitakari OT, Rimm EB, Rioux JD, Rizzi F, Rudan I, Salomaa V, Sever PS, Shields DC, Shuldiner AR, Sinisalo J, Stanton AV, Stolk RP, Strachan DP, Tardif J-C, Thorsteinsdottir U, Tuomilehto J, Veldhuisen DJV, Virtamo J, Viikari J, Vollenweider P, Waeber G, Widen E, Cho YS, Olsen JV, Visscher PM, Willer C, Franke L, G.Bp. Consortium, Cardi. Consortium, Erdmann J, Thompson JR, P.G. Consortium, Pfeufer A, Q.G. Consortium, Sotoodehnia N, Q.-I. Consortium, Newton-Cheh C, Consortium C-A, Ellinor PT, Stricker BHC, Metspalu A, Perola M, Beckmann JS, Smith GD, Stefansson K, Wareham NJ, Munroe PB, Sibon OCM, Milan DJ, Snieder H, Samani NJ, Loos RJF, Identification of heart rate-associated loci and their effects on cardiac conduction and rhythm disorders., Nat. Genet. 45 (2013) 621–631. 10.1038/ng.2610. [PubMed: 23583979]

[71]. Iop L, Iliceto S, Civieri G, Tona F, Inherited and Acquired Rhythm Disturbances in Sick Sinus Syndrome, Brugada Syndrome, and Atrial Fibrillation: Lessons from Preclinical Modeling, Cells. 10 (2021) 3175, 1–52. 10.3390/cells10113175.

[72]. Cai S, Zheng L, Yao Y, Selection of patients with symptomatic vagal-induced sinus node dysfunction: Who will be the best candidate for cardioneuroablation?, Front Physiol. 14 (2023) 1088881. 10.3389/fphys.2023.1088881. [PubMed: 36824466]

[73]. Kusumoto FM, Schoenfeld MH, Barrett C, Edgerton JR, Ellenbogen KA, Gold MR, Goldschlager NF, Hamilton RM, Joglar JA, Kim RJ, Lee R, Marine JE, McLeod CJ, Oken KR, Patton KK, Pellegrini CN, Selzman KA, Thompson A, Varosy PD, 2018 ACC/AHA/HRS Guideline on the Evaluation and Management of Patients With Bradycardia and Cardiac Conduction Delay A Report of the American College of Cardiology/American Heart Association Task Force on Clinical Practice Guidelines and the Heart Rhythm Society, J Am Coll Cardiol. 74 (2019) e51–e156. 10.1016/j.jacc.2018.10.044. [PubMed: 30412709]

[74]. Acharya R, Shrestha R, A. R, S. R, Postpartum Transient Hypervagotonic Sinus Node Dysfunction Leading to Sinus Bradycardia: A Case Report, Cureus J Medical Sci. 12 (2020) e9186. 10.7759/cureus.9186.

[75]. Park H-W, Cho J-G, Yum J-H, Hong Y-J, Lim J-H, Kim H-G, Kim J-H, Weon-Kim Y-K Ahn, Jeong M-H, Park J-C, Kang J-C, Clinical Characteristics of Hypervagotonic Sinus Node Dysfunction, Korean J Intern Medicine. 19 (2004) 155–159. 10.3904/kjim.2004.19.3.155.

[76]. Mc R) H1253–H1266. 10.1152/ajpheart.00734.2012.

[77]. Lv Z, Hu M, Fan M, Li X, Lin J, Zhen J, Wang Z, Jin H, Wang R, Podocyte-specific Rac1 deficiency ameliorates podocyte damage and proteinuria in STZ-induced diabetic nephropathy in mice, Cell Death Dis. 9 (2018) 342–357. 10.1038/s41419-018-0353-z. [PubMed: 29497040]

[78]. Desjardins CA, Naya FJ, The Function of the MEF2 Family of Transcription Factors in Cardiac Development, Cardiogenomics, and Direct Reprogramming, J Cardiovasc Dev Dis. 3 (2016) 26–58. 10.3390/jcdd3030026. [PubMed: 27630998]

[79]. Ago T, Liu T, Zhai P, Chen W, Li H, Molkentin JD, Vatner SF, Sadoshima J, A Redox-Dependent Pathway for Regulating Class II HDACs and Cardiac Hypertrophy, Cell. 133 (2008) 978–993. 10.1016/j.cell.2008.04.041. [PubMed: 18555775]

[80]. Zhang D, Hu X, Li J, Hoogstra-Berends F, Zhuang Q, Esteban MA, de Groot N, Henning RH, Brundel BJJM, Converse role of class I and class IIa HDACs in the progression of atrial

fibrillation, J Mol Cell Cardiol. 125 (2018) 39–49. 10.1016/j.yjmcc.2018.09.010. [PubMed: 30321539]

Highlights

- The loss of p21-activated kinase (Pak1) results in sinoatrial node (SAN) bradycardia.
- Pak1 regulates the SAN pacemaker's membrane clock component by attenuating class II HDAC4 activity.
- During atrial fibrillation (AF), the downregulation of Pak1 can contribute to SAN bradycardia through the activation of ERK1/2 signaling.

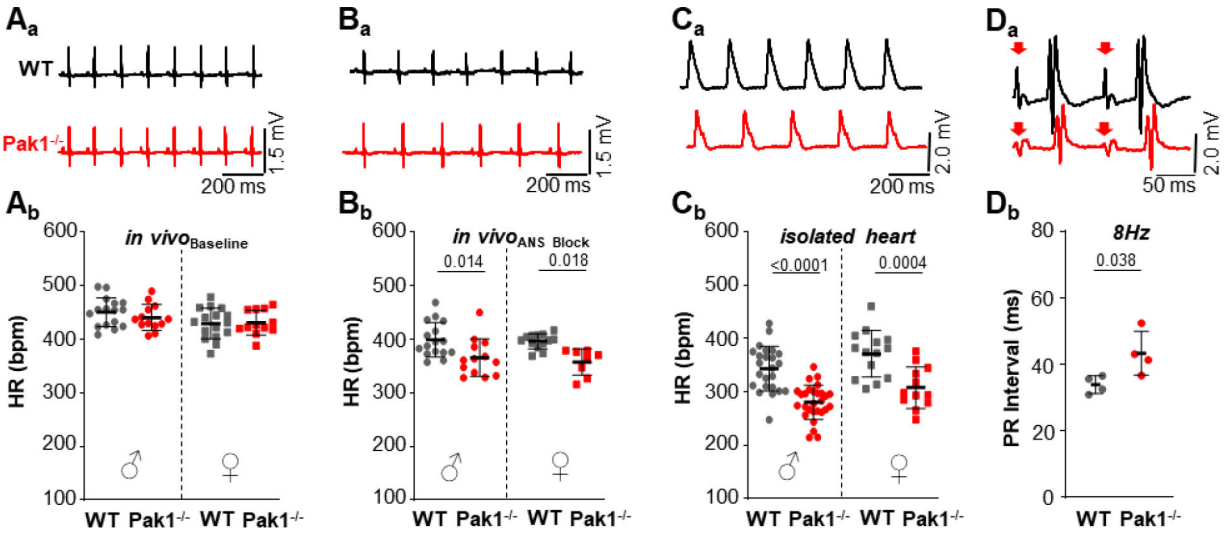

Figure 1. Loss of Pak1 attenuates the intrinsic heart rate (HR) in male and female mice.

Representative recordings from male (●) and female (■) WT (n: ●=16, ■=16) and Pak1$^{-/-}$ (n: ●=13, ■=12) mice showing (A$_a$) ECGs in control conditions and (B$_a$) after suppression of autonomic signaling (atropine: 1 mg/kg + propranolol: 1 mg/kg), (n: ●=16, ■=13, ●=13, ■=8), (Ca) atrial electrograms from isolated hearts (n: ●=24, ■=14, ●=28, ■=12) as well as (*D*a) ECGs from isolated hearts paced at 8Hz (n: ●=4 ●=4), red arrows indicate the stimulation artifact. Quantification of the heart rate (HR) under the described conditions is shown in A$_b$ - C$_b$, respectively. Quantification of the PR interval in isolated hearts is shown in D$_b$. Data are presented as mean ± SD. One-Way ANOVA.

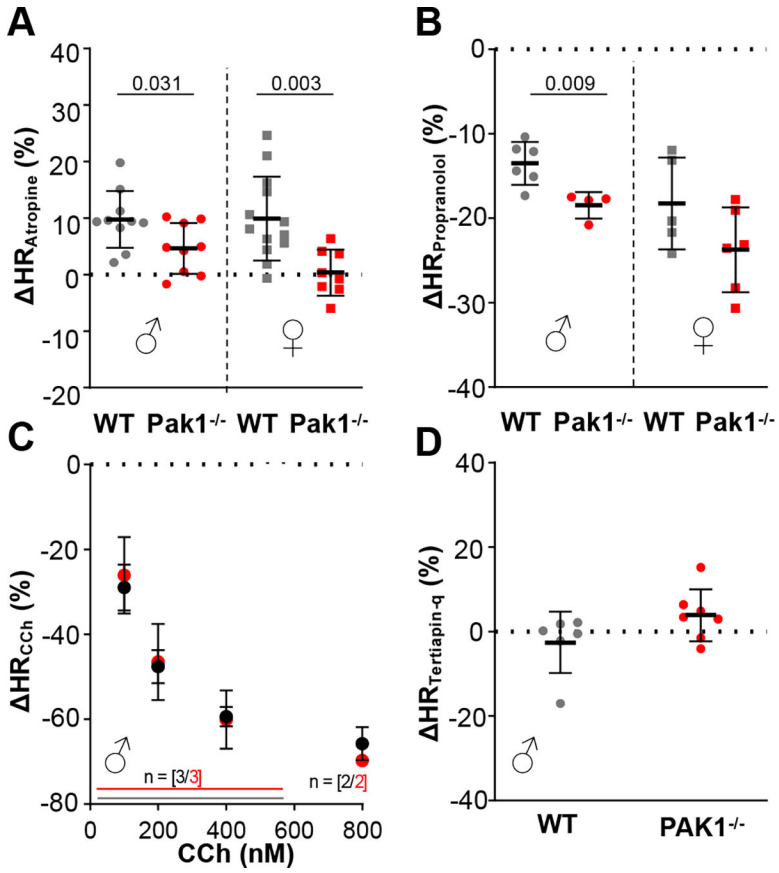

Figure 2. Alterations in ANS signaling mask the attenuated HR in Pak1$^{-/-}$ mice:

Quantification of the percentage change in HR in male (●) and female (■) WT (n: ●=10, ■=13) and Pak1$^{-/-}$ (n: ●=9, ■=8) mice in response to the suppression of (**A**) parasympathetic (atropine) and (**B**) sympathetic signaling (propranolol) (n: ●= 6, ●=4, ■= 5, ■=6). Percent change in HR of isolated male WT and Pak1$^{-/-}$ hearts in response to perfusion with (**C**) crescent CCh concentrations (sample size indicated in the figure for each CCh concentration) or (***D***) *a* blocker of GIRK, TerQ (n: ●=6 and ●=7). Data are means ± SD. Student's *t* test (*A, C - D*) and Mann-Whitney test (*B*).

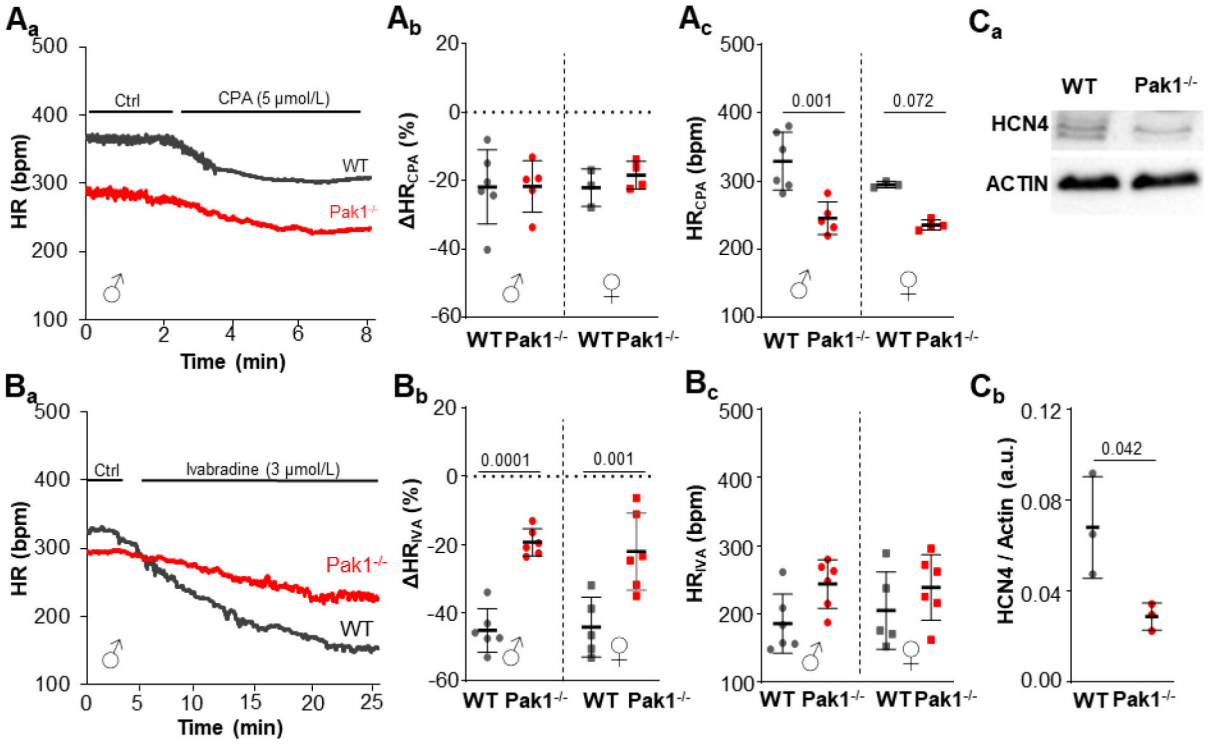

Figure 3: Loss of Pak1 attenuates the contribution of the voltage clock to pacemaker activity.

Representative HR recordings from isolated, Langendorff perfused male and female WT (●, ■) and Pak1$^{-/-}$ (●, ■) hearts during (**A**) superfusion with the SERCA inhibitor CPA or (**B**) the HCN4 inhibitor IVA. Summary data of CPA and IVA induced percent change in HR, respectively (**A$_b$**, n: ●=6, ●= 5, ■=3, ■= 4) and (**B$_b$**, n: ●=6, ●=6, ■=5, ■=6) as well as absolute HR in CPA (**Ac,** n: ●=6, ●=5, ■=3, ■=4) or IVA (**Bc**, n: ●=6, ●=6, ■=5, ■=6). Representative Western blot displaying HCN4 protein levels (**Ca**) and quantification of HCN4 protein levels normalized to actin expression (**C$_b$**). Data are means ± SD. One-Way ANOVA (A –B) Student's *t* test (C).

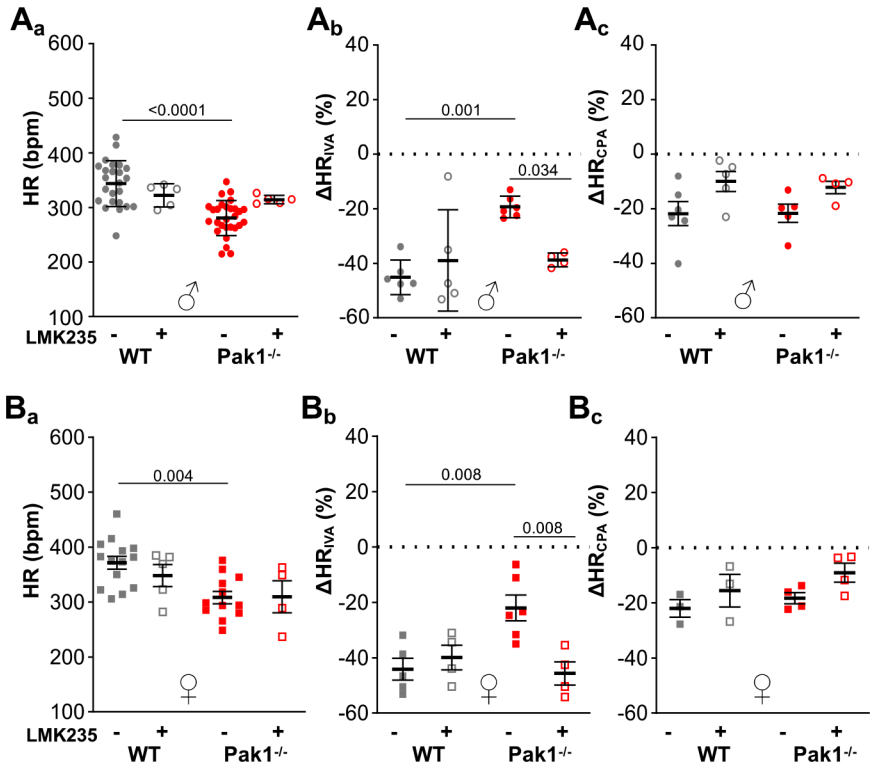

Figure 4: Pak1 controls HCN contribution to pacemaker activity through class II HDACs.

HR analysis in male and female WT (●, ■) and Pak1$^{-/-}$ (●, ■) Langendorff perfused hearts under control conditions and after treatment of mice with LMK (WT: ◯, □; Pak1$^{-/-}$: ◯,). Quantification of the basal HR (♂: **A_a**, n: ●= 24, ◯=5, ● =28, ◯=5) (♀: **B_a**, n: □=14, □=5, ■=12, □=4) and the percentage change in HR after perfusion with IVA (♂: **Ab,** n: ●=6, ◯=5, ● =6, ◯=4) (♀: **Bb**, n: =5, =4, =6, =4) or CPA (♂: **Ac,** n: ●=6, ◯=5, ● =5, ◯=4) and (♀: **B_c**, n: =3, =3, =4, =4). Data are presented as means ± SD. One Way ANOVA.

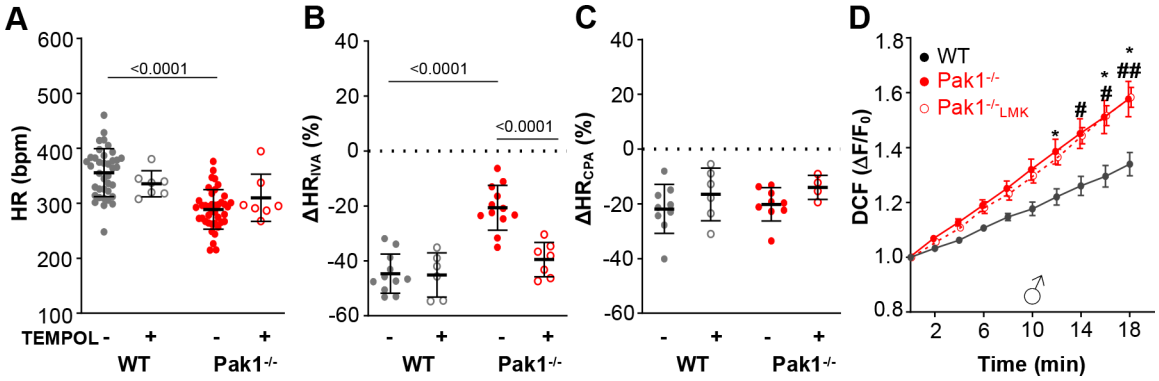

Figure 5. ROS-dependent regulation of HCN contribution to pacemaker activity.

HR analysis in WT (●) and Pak1$^{-/-}$ (●) Langendorff perfused hearts under control conditions and after treatment of mice with TEMPOL (WT: ◯; Pak1$^{-/-}$:). Quantification of the basal HR (**A,** n: ●= 38, ◯=7, ● =40, ◯=7) and percentage change in HR after perfusion with IVA (**B,** n: ●= 11, ◯=6, ● =12, ◯=7) or CPA (**C,** n: ●= 9, ◯=6, ● =9, ◯=4). (**D**) Change of cellular DCF fluorescence over time in atrial myocytes isolated from WT (●, n of cells/mice = 7/3, Pak1$^{-/-}$ (●, n = 10/3) or Pak1$^{-/-}$ hearts from mice treated with LMK2335 (◯, n = 7/2). Data are presented as means ± SD. One Way ANOVA (A –C), Nested ANOVA (D). * represents WT vs Pak1$^{-/-}$, where $p<0.05$ *; # represents Pak1$^{-/-}$ vs Pak1$^{-/-}$ LMK, where $p<0.05$ $^{\#}$; $p<0.01^{\#\#}$.

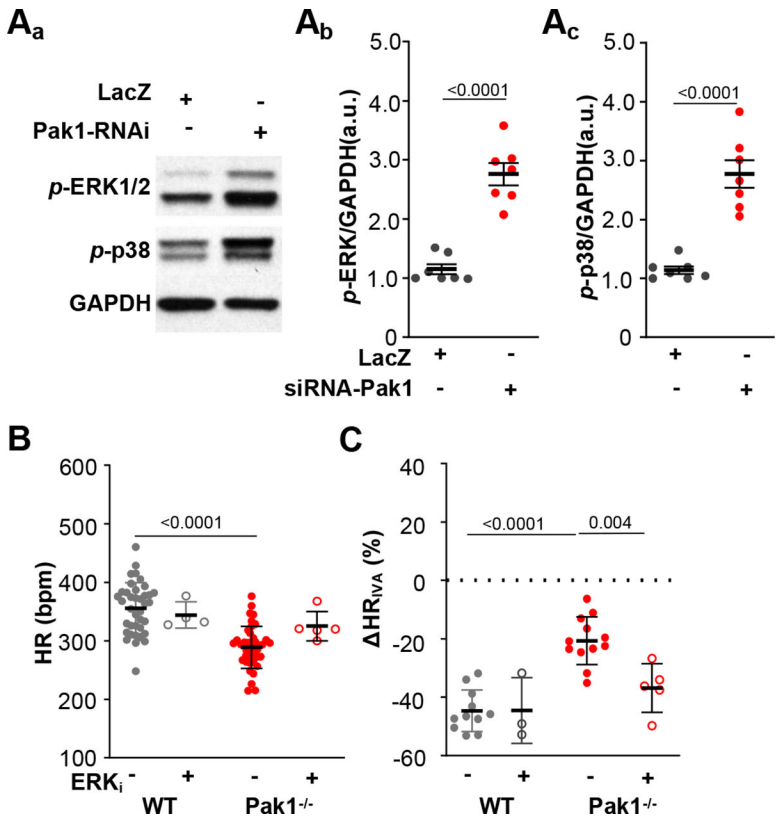

Figure 6: Attenuation of Pak1 promotes increased activity of ERK and p38:

Representative Western blots displaying *p*-ERK1/2 and *p*-p38 levels in protein lysate from HL-1 cells after (**A_a**, n = 7/group) adenoviral gene transfer of LacZ or Pak1-siRNA. *P*-ERK1/2 **($A_{b)}$** and *p*-p38 **(A_c)** protein levels normalized to GAPDH expression. Summary of experimental results from Langendorff perfused WT (●) and $Pak1^{-/-}$ (●) hearts under control conditions or after treatment with SCH772984 (ERKi; ◯, ◯). HR after ERKi treatment (**B,** n: ●=38, ◯=4, ● =40, ◯=5) and the IVA induced change in HR (**C,** n: ● =11 ◯=3 ● =12, ◯=5). Data are presented as mean ± SD. Student's *t* test (A-B) and One Way ANOVA (C-D).

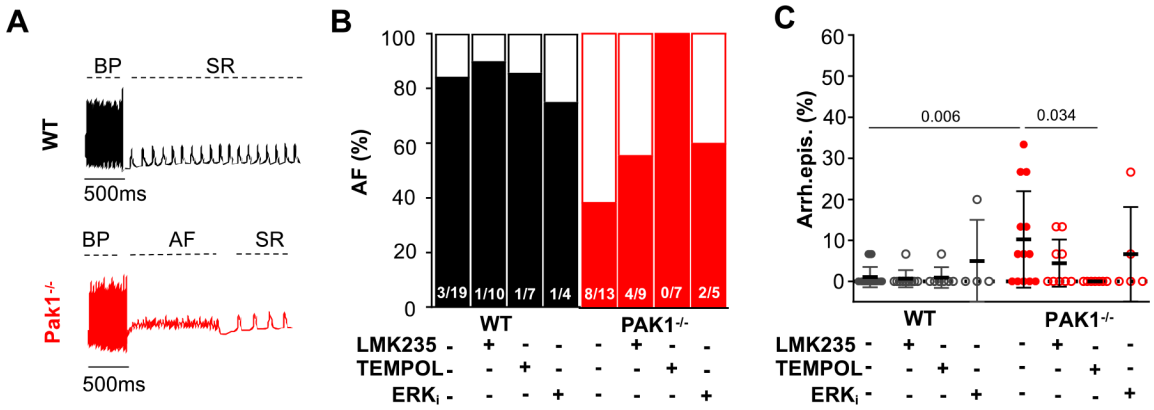

Figure 7. ROS but not SAN bradycardia promotes atrial arrhythmia in Pak1$^{-/-}$ hearts.

A: Representative traces of atrial electrograms showing the recovery of sinus rhythm (SR) after burst pacing (BP) in WT (black) and Pak1$^{-/-}$ (red) hearts. ***B*:** Percentage of WT and Pak1$^{-/-}$ animals with AF (□, □) or SR (■, ■) after BP. ***C***: Percentage of BP episodes eliciting AF/heart during control conditions (●=19, ●=13) and after LMK235 (◯=10, ◯=9), TEMPOL (◯=7, ◯=7) or SCH772984 (ERK_i) (◯=4, ◯=5) treatment. Data are presented as mean ± SD. One Way ANOVA (**C**)